SYNTHESIS OF ANTHRACENE-BASED MACROCYCLE FOR DETECTION OF EXPLOSIVES

A THESIS SUBMITTED TO
THE GRADUATE SCHOOL OF NATURAL AND APPLIED SCIENCES
OF
MIDDLE EAST TECHNICAL UNIVERSITY

BY

TUĞÇE YILMAZ

IN PARTIAL FULFILLMENT OF THE REQUIREMENTS
FOR
THE DEGREE OF MASTER OF SCIENCE
IN
CHEMISTRY

JANUARY 2019

Approval of the thesis:

SYNTHESIS OF ANTHRACENE-BASED MACROCYCLE FOR DETECTION OF EXPLOSIVES

submitted by **TUĞÇE YILMAZ** in partial fulfillment of the requirements for the degree of **Master of Science in Chemistry Department, Middle East Technical University** by,

Prof. Dr. Halil Kalıpçılar
Dean, Graduate School of **Natural and Applied Sciences** _____

Prof. Dr. Cihangir Tanyeli
Head of Department, **Chemistry** _____

Assist. Prof. Dr. Salih Özçubukçu
Supervisor, **Chemistry, METU** _____

Examining Committee Members:

Prof. Dr. Cihangir Tanyeli
Chemistry, METU _____

Assist. Prof. Dr. Salih Özçubukçu
Chemistry, METU _____

Prof. Dr. Mürvet Volkan
Chemistry, METU _____

Assoc. Prof. Dr. Emrullah Görkem Günbaş
Chemistry, METU _____

Assist. Prof. Dr. Safacan Kölemen
Chemistry, Koç University _____

Date: 11.01.2019

I hereby declare that all information in this document has been obtained and presented in accordance with academic rules and ethical conduct. I also declare that, as required by these rules and conduct, I have fully cited and referenced all material and results that are not original to this work.

Name, Surname: Tuğçe Yılmaz

Signature:

ABSTRACT

SYNTHESIS OF ANTHRACENE-BASED MACROCYCLE FOR DETECTION OF EXPLOSIVES

Yılmaz, Tuğçe
Master of Science, Chemistry
Supervisor: Assist. Prof. Dr. Salih Özçubukçu

January 2019, 57 pages

Development of fluorescent sensors for detection of explosives become very interesting area for researchers. Picric acid is an important member of nitro-aromatic compounds which is also a powerful explosive. Fluorescent sensors are one of the essential way to detect picric acid, since they have many advantages, such as high sensitivity, simple instrumentation, and quick response.

Cyclophanes are molecules that their cyclic structure makes them very promising candidate for molecular recognition. Anthracene-based cyclophanes exhibit strong fluorescence quenching with the interaction of electron deficient molecules.

In this thesis, anthracene-based macrocycle was synthesized and its sensor ability was tested for picric acid determination. It was found that anthracene-based macrocycle is quite selective for picric acid and 2,4-DNP. Stern-Volmer quenching constants were found to be 5.28x104 M-1 for picric acid and 5.61x104 M-1 for 2,4-DNP. Detection limits were calculated and found to be 0.39 μM for PA and 0.25 μM for 2,4-DNP. The comparison of quenching constant, detection limit, and media used for picric acid detection with some recent reports in the literature were studied.

Keywords: Fluorescent sensors, Explosives, Anthracene-based macrocycle, Picric acid.

ÖZ

PATLAYICILARIN TAYİNİ İÇİN ANTRASEN BAZLI MAKROMOLEKÜL SENTEZİ

Yılmaz, Tuğçe
Yüksek Lisans, Kimya
Tez Danışmanı: Dr. Öğr. Üyesi Salih Özçubukçu

Ocak 2019, 57 sayfa

Patlayıcıların tespit edilmesi için floresans sensörlerin gelişimi araştırmacılar için ilgi çekici hale gelmiştir. Yüksek duyarlılık, kolay ölçülebilirlik, ve hızlı yanıt verme süresi gibi birçok avantaja sahip olmalarından dolayı floresans sensörler, pikrik asit tayini için kullanılan etkili yöntemlerden biridir.

Halkalı yapıları sayesinde siklofanlar moleküler tanıma için umut vaat eden moleküllerdir. Antrasen bazlı siklofanlar ise elektronca fakir moleküller ile etkileşerek güçlü bir floresans sönümlenmesi gerçekleştirirler.

Bu çalışmada, antrasen bazlı siklofan molekülü sentezlenmiş ve pikrik asit tayini için sensör özelliği incelenmiştir. Antrasen bazli siklofan bileşiğinin pikrik asite ve 2,4-DNP'te seçici olduğu bulunmuştur. Stern-Volmer sönümlenme sabiti pikrik asit için 5.28x104 M-1 ve 2,4-DNP için 5.61x104 M-1 bulunmuştur. Tespit limiti pikrik asit için 0.39 μM ve 2,4-DNP için 0.25 μM olarak hesaplanmıştır. Sönümlenme sabitinin, tespit limitinin ve pikrik asit tayininde kullanılan çözücü ortamının güncel literatür ile karşılaştırması yapılmıştır

Anahtar Kelimeler: Floresans sensörler, Patlayıcılar, Antrasen bazlı halkalı yapı, Pikrik asit.

To my beloved brother H. Alper Yılmaz

ACKNOWLEDGMENTS

I would like to express my gratitude to my supervisor Assist. Prof. Dr. Salih Özçubukçu for his precious guidance and encouragement. It would have been impossible for me to conclude this work without his patience and invaluable advices. It has been a great honor for me to be a part of his research group as a graduate student.

I also would like to thank every single member of Özçubukçu Research group, Dr. Aytül Saylam, Güzide Aykent, Burcu Okyar, Muzaffer Gökçe, Mehmet Seçkin Kesici, Volkan Dolgun, and Medine Soydan for their precious friendship, advices and helps.

I wish to thank NMR specialist Betül Eymur for NMR analysis in our department and Prof. Dr. Ahmet Önal for giving me the opportunity to use the spectrofluorometer.

I would like to thank BAP for financial support.

A special thanks to my friends Halime Serinçay and Nilüfer Kara for their priceless friendships.

Also, I would like to thank my fiance Barış Kaçaroğlu for his love, and support.

Finally, I would thank my family, Sebahattin Yılmaz, Aysel Yılmaz, and Habil Alper Yılmaz for their endless love, support, and patience. This thesis would not have been possible without them. Thank you for everything.

.

TABLE OF CONTENTS

LIST OF TABLES

TABLES

LIST OF FIGURES

FIGURES

LIST OF SCHEMES

SCHEMES

LIST OF ABBREVIATIONS

ABBREVIATIONS

NADH: Nicotinamide adenine dinucleotide

PA: Picric Acid

TNT: Trinitrotoluene

HMTA: Hexamethylenetetramine

AcOH: Acetic Acid

HEPES: 4-(2-Hydroxyethyl)piperazine-1-ethanesulfonic acid

SD: Standart Deviation

DL: Detection Limit

CHAPTER 1

INTRODUCTION

1.1. Sensors

Our way of life improves the advancement of applied science. Sensing technology has a great contribution on the expanding research technology. A sensor is a system which provides a measurable signal with the interaction of matter or energy. Signals can be classified according to its electrical domain. Six type/form of energy is accepted in the field of instrument systems. These are radiant, mechanical, thermal, electrical, magnetic, and chemical energies[1].

1.2. Chemical Sensors

A chemical sensor is a device that produces a detectable signal at any desired concentration. A transducer and a receptor are two main components of a system. In the receptor of a sensor, the information from a physical change, a chemical reaction, and a biochemical process is transformed into a type of energy that gives rise to an analytical signal. The transducer component is intended for direct analysis about the nature of chemical composition.

1.2.1. Classification of Chemical Sensors

Chemical sensors can be classified based on the working principle of the transducer[2]. These are listed in the Table 1.1.

Table 1.1. *Classification of Chemical Sensors*

Optical	Absorbance, Reflectance, Luminescence, Fluorescence, Refractive Index, Optothermal Effect, Light Scattering
Electrochemical	Voltammetric, Potentiometric, CHEMFET, Potentiometric Solid Electrolyte Gas Sensors
Electrical	Metal Oxide Semiconductor Sensors, Organic Semiconductor Sensors, Electrolytic Conductivity Sensors, Electric Permittivity Sensors
Mass Sensitive	Piozoelectric Devices, Surface Acoustic Wave Devices
Magnetic	Oxygen Monitors
Thermometric	Optothermal Effects
Other Physical Properties	X^-, β^-, Γ^- Radiation

1.3. Fluorescence

Fluorescence sensing has an important place in biological and chemical sciences. To illustrate the physics of luminescence, the Jablonski diagram is used. In Figure 1.1, molecular fluorescence lifetime can be seen on a time scale of nanoseconds. As a result of fast response, fluorescence spectroscopy is used as an essential method by scientist from many disciplines for high sensitive and selective detection[3].

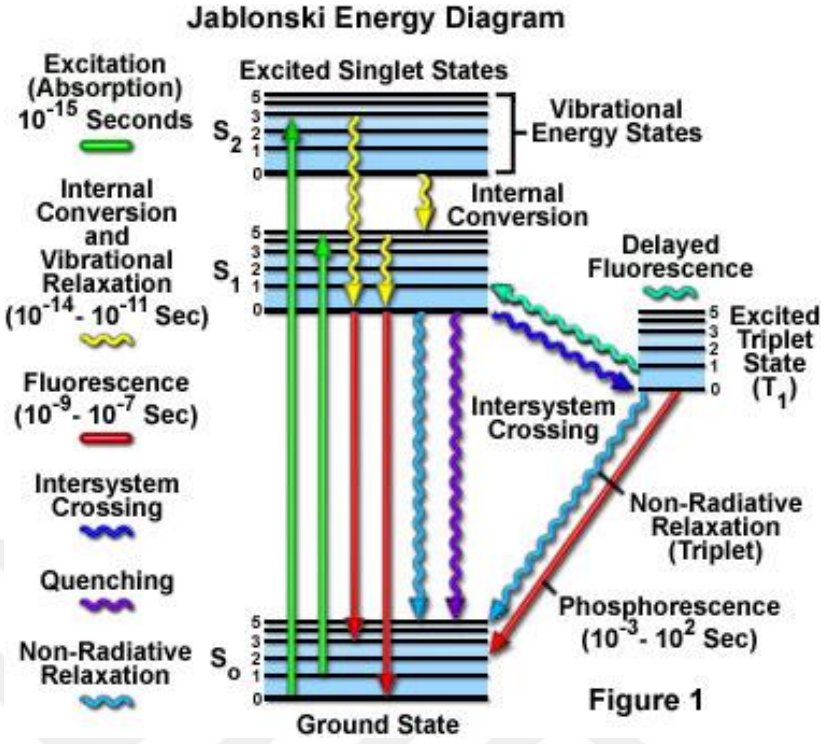

Figure 1.1. Jablonski energy diagram[3].

1.3.1. Fluorophores

Fluorescence probe is the type of fluorescent substance that can absorb and emit the light of a specific wavelength region. For a given fluorochrome, the absorption and emission spectra determine the intensity of fluorescence. Fluorophores are generally used for cellular imaging and single-molecule detection.

Proteins GFP, YFP, and RFP; aromatic amino acids tryptophan (trp), tyrosine (tyr), and phenylalanine (phe); enzyme cofactors NADH, flavins, derivatives of pyridoxyl, and chlorophyll; and dyes dansyl, fluorescein, and rhodomine are some of the molecules that can be used as fluorophore (Figure 1.2)[3].

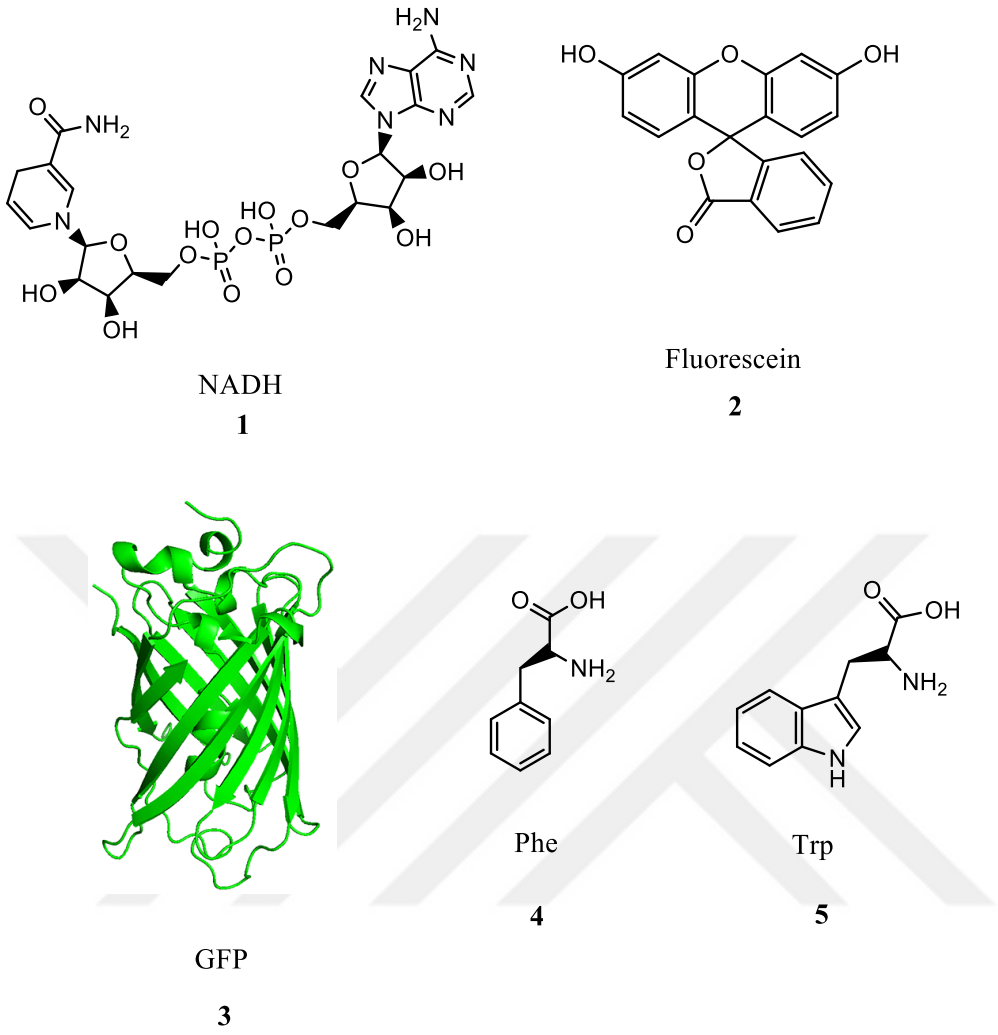

Figure 1.2. Structures of some typical fluorophores[3].

1.4. Fluorescent Sensors

With the increasing number of fluorescence-based sensing probes in the growing area of imaging techniques allow the sensitive detection of various targets. These targets could be metal ions[4] (e.g. Fe^{2+}, Fe^{3+}, Zn^{2+}, Mn^{2+}, and Pb^{2+}); small organic molecules (e.g. ascorbic acid[5], and glucose[6]); explosives (e.g. picric acid[7], RDX[8], and TNT[9]) and biomolecules such as proteins[10], enzymes[11] and organelles[12].

Metal ions are known to play an essential role on all life forms. For this reason, analytical techniques used for the determination of metal ions become crucial.

Fluorescence detection comes into prominence due to shorter response time and lower cost. Ca^{2+} ion is the most preferred target of fluorescent probes. The function of calcium has great importance in living organism. Many cellular processes such as regulation and signaling are regulated/are controlled by calcium. In a research done by Tsien and coworkers in 1980 for the first time, quin2[13], fura-2[14], fluo-3[15], and rhod-2[15] were used as a chelating agent for Ca^{2+} ion detection (Figure 1.3). In 2011, another research done by Takuya Terai's and Koji Suzuki's group shows that NIR fluorescent probes have high activity and these probes should be beneficial for monitoring calcium ion fluctuation in tissues[16].

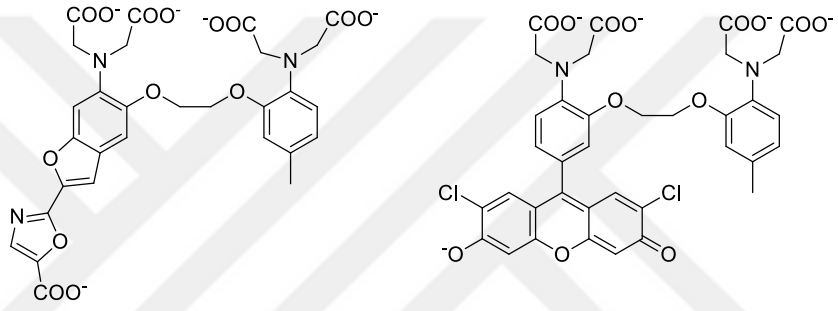

fura-2 **6** fluo-3 **7**

Figure 1.3. Fluorescent probes for Ca^{2+} ion[14,15].

Detection of biomolecules is one of the most essential part of biomedical analysis. Proteins take a significant place in the clinical studies. Invention of drugs, diagnosis of diseases, and tissue engineering are important applications that researchers offer to the developing field. Ewa and Tomasz Heyduk have proposed[10] aptamer-based fluorescence sensor for detecting proteins. The fluorophore-labeled oligonucleotides attached to the aptamer results a change of fluorescence signal.

1.5. Anthracene

Anthracene is a solid aromatic hydrocarbon obtained from coal tar. Three fused benzene rings are attached to the molecule. Anthracene is easily transformed into an oxidized form anthraquinone. Anthracene as a fluorophore excites at 360-400 nm and the emission wavelenght is between 400-600 nm[17].

Anthracenes have been used in many field such as material chemistry, medicine, and biological systems. Pseudourea was the first anthracene-based drugs examined in clinical tests/studies (Figure 1.4)[18]. Anthracyclines are another example of anthracene derivatives that exhibit good activity against tumor cells by preventing accelerated growth[19]. The planarity of anthracene gives to three-ring system the ability to match with the DNA base pairs. 9,10-substituted anthracene derivatives are useful for polymeric films to provide good optical quality. Also, they are used as blue light-emitting molecules for OLED devices[20].

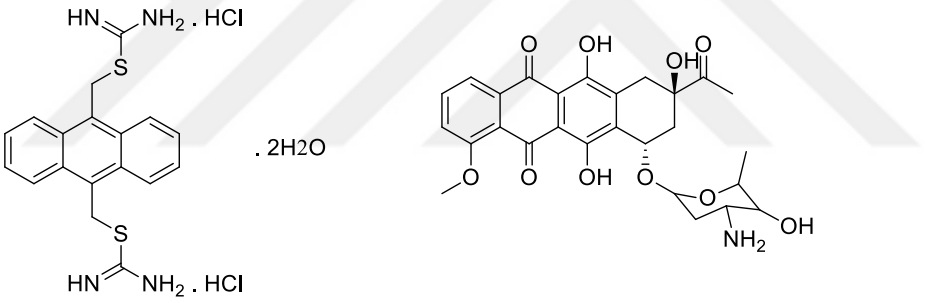

Pseudourea **8**

Anthracyclines **9**

Figure 1.4. Anthracene derivatives[19].

1.6. Anthracene-Based Fluorescent Sensors

The stability of anthracene ring and the ability of high luminescence make the molecule good choice for fluorescence sensing.

Organic near-infrared (NIR) dyes have many applications such as solar cells, laser technology, bioimaging, and biolabeling. The intense penetration capacity, low light

scattering, and low background interference make them preferred/preferable fluorescence probe in the visible region. In order to increase photostability, 4,4-Difluoro-4-bora-3a,4a-diaza-*s*-indicane, known as boron dipyrromethene (BODIPY), is used as a fluorescent fluorophore. In 2011, an intramolecular oxidative cyclodehydrogenation reaction between an anthracene molecule and a boron dipyrromethene (BODIPY) took place to form perylene and –porphyrin-fused BODIPY dyes (Figure 1.5). These dyes both monomer and dimer are performed high photostability. By the help of an appropriate geometry and electronic structure anthracene unit is quite fit the zigzag edge of a BODIPY scaffold. The anthracene-fused BODIPY dyes could find functional applications in organic field-effect transistors and dye-sensitized solar cells[21].

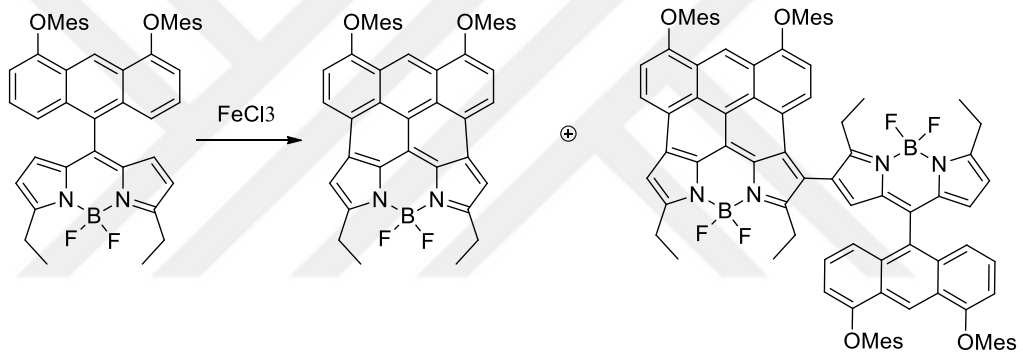

Figure 1.5. Anthracene-fused BODIPY Dyes[21].

Phosphate groups have significant importance in biological processes. Their high abundancy makes these species useful for sensor and receptor systems. Adenosine 5'-triphosphate (ATP), adenosine 5'-diphosphate (ADP) and adenosine 5'-monophosphate (AMP) are essential nucleotides that contain one or more phosphate anions. Nucleoside triphosphates, particularly ATP, are the main source of energy in living systems. ATP has some important role in the cell such as active transport, cell signaling, muscle contraction, and synthesis of DNA and RNA.[22] ADP and AMP also perform their function in metabolism, transformation of genetic information, and bioenergetics. Many kinases and ATPases catalyzed biological reaction give ADP as

a mutual product. Additionally, higher amount of inorganic pyrrophosphate (PPi) production by biosynthetic reaction attracts the attention to phosphate anion to design chemosensors for these phosphates.[23] Cyclophanes are cyclic compounds which contain sufficient holes to recognize guest molecules. According to a recent study, nucleotide detection by using anthracene-based cyclophanes shows promising results[24,25]. In 2014, Ping Hu and co-workers were reported[26] to develop an efficient sensor for anion in neutral aqueous media. They proposed that anthracene based mono nuclear and dinuclear zinc complexes provide sensitivity for nucleoside polyphosphates (Figure 1.6). Metal coordinated cyclophane binds the ATP, ADP, AMP, and PPi via strong π-π stacking interactions. Due to the fact that ATP has more negative charge, its binding affinity higher than the other phosphate species. ADP, on the other hand, shows the most intense fluorescence response owing to the well-suited distance between host and guest molecule[26].

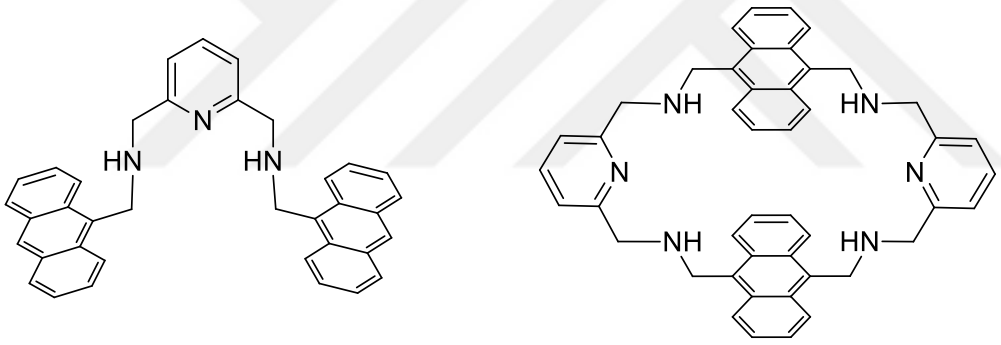

13 **14**

Figure 1.6. Anthracene-based (mono and dinuclear) zinc complexes[26].

1.7. Explosive Sensors

For the last ten years, many research groups focus their attention on detecting of nitro-aromatic compounds. These molecules are used in numerous field, such as dye industry, pharmaceuticals, rubber products, explosives, rocket fuels, pesticides, and chemical laboratories[27]. However, for all wide field of application, environmental pollution is caused by nitro-aromatic compounds as a waste of industrial product and consequently many health problems come into existence. 2,4,6-trinitrotoluene (TNT)

and 2,4,6-trinitrophenol (picric acid, PA) are well-known explosives among nitro-aromatic compounds. Their hazardous effect to human body leads the scientists to design effective explosive sensors. Several methods have been applied for detecting the nitro-aromatic explosives. GC-MS, ion-mobility spectroscopy (IMS), Raman spectroscopy, cyclic voltammetry, liquid Chromatography-mass spectrometry (LC-MS), and photoluminescence spectroscopy (PL) are common techniques to detect many explosives including PA[28,29]. Fluorescence sensing has recently come into prominence due to quick response, easy sample preparation, sensitivity, and selectivity.

In 2016, Dr. Joshi and co-workers achieved to synthesis a fluorescent benzimidazolium-based sensor for selective detection of picric acid in aqueous media[30]. Coumarin is used as a fluorescent molecule in this study since coumarin-derivatives emit the light in visible region and their toxicity are very low among other fluorophores. They also demonstrated that coumaryl linked benzimidazolium salt was able to behave like turn-off fluorescence probe in the presence of aromatic/nonaromatic compounds (Figure 1.7).

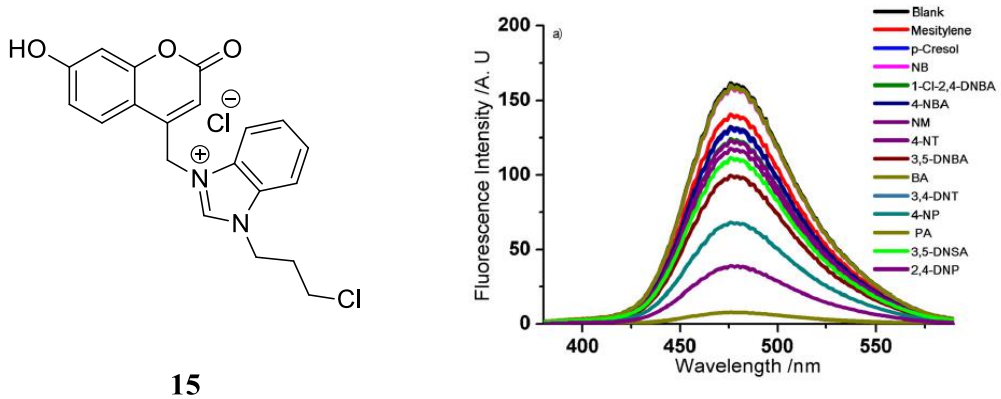

Figure 1.7. Fluorescent benzimidazolium probe and its turn off behavior[30].

Another study of Dr. Dhir, Dr. Krishnan, and co-workers in 2018, Ni-Anthracene complex was used to obtain selective and sensitive detection of picric acid (Figure 1.8). By choosing an anthracene derivative as a fluorescent probe, they intended to

take advantage of electron rich moiety of aromatic group. Thus, electron deficient nitro-aromatic compounds can exhibit effective π- π stacking interaction with electron rich fluorescent molecule. As a result of this interaction, quenching the emission intensity of fluorophore occurs by the 2,4,6-trinitrophenol (TNP). They observed high selectivity towards picric acid via fluorescence titration studies among other nitro-compounds, as follows nitrotoluene (NT), 2,4-dinitrotoluene (2,4-DNT), 1,4-dinitrobenzene (1,4-DNB), and anions (F^-, Cl^-, Br^-, I^-, OH^-, HSO_3^-, CN^-, NO_3^-, CH_3COO^-, ClO_4^-, and PO_4^-)[31].

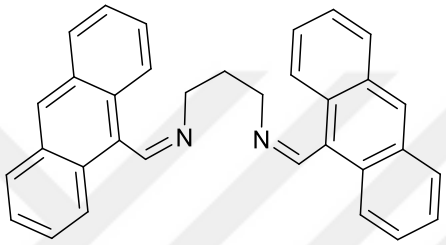

16

Figure 1.8. A Ni-Anthracene complex for detecting of picric acid[31].

1.8. Biosensors

Biosensors are devices that have biological recognition part. Biological response from this part is converted into an electrical signal. There are several types of biosensors, such as enzyme-based, tissue-based, immunosensors, DNA biosensors, and thermal band piezoelectric biosensors. Biosensors have been applied several areas namely food industry, medical field, marine sector[32,33].

Glucose biosensors have great importance in the biosensing market due to their high sensitivity, selectivity, and quick analytical response. Conjugated polymers (CPs) are one of the alternative way to design glucose sensor. Peptides are important molecules that are widely used in medicinal chemistry, drug delivery system, and biosensors application. Conjugation of the peptide to monomers by choosing polar side chains such as aspartic acids, glutamic acids, and arginine would increase the solubility of

corresponding polymers in water. Peptide conjugation to monomers are also versatile alternative for the immobilization of enzymes with the polymerized monomers[34].

1.9. Aim of the Study

1.9.1. Antracene-based macrocycle for detection of explosives

A selective detection of explosives is desired by many scientists since they have serious effect on public security and human body. Increasing health problems, rising terror attacks, and polluted environment are main/basic reasons to motivate researchers to design practical probes. As it mentioned above, these probes/they have widespread application field. Anthracene derivatives are good choice as a fluorophore, due to their electron rich moiety makes them very promising candidate for strong fluorescence quenching. Also, cyclic structure of donor molecule makes a suitable cavity for better interaction with electron deficient molecule.

In view of this information, our aim is to synthesize anthracene-based macrocycle to detect picric acid selectively, and investigate the interactions and the selectivity studies performed by spectrofluorometer using fluorescence property of anthracene moiety.

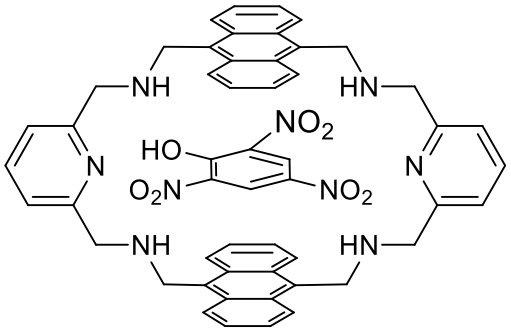

17

Figure 1.9. Anthracene-based macrocycle for detection of explosives.

1.9.2. Peptide SNS-type monomer conjugates for detection of glucose

A selective and sensitive detection of glucose molecule is gaining popularity in the biosensing market for the early diagnosis and the detection of diabetes[34]. Conjugated polymers have a tendency to increase the stability and sensitivity of biomolecules. Peptides are molecules that are used peptide-polymer conjugates and they attained different structure by choosing proper amino acids, such as arginine, and glutamic acid to increase water solubility.

In view this information, our aim is to synthesize water soluble SNS-type carboxylic acid group containing two different peptides for selective and sensitive detection of glucose molecule.

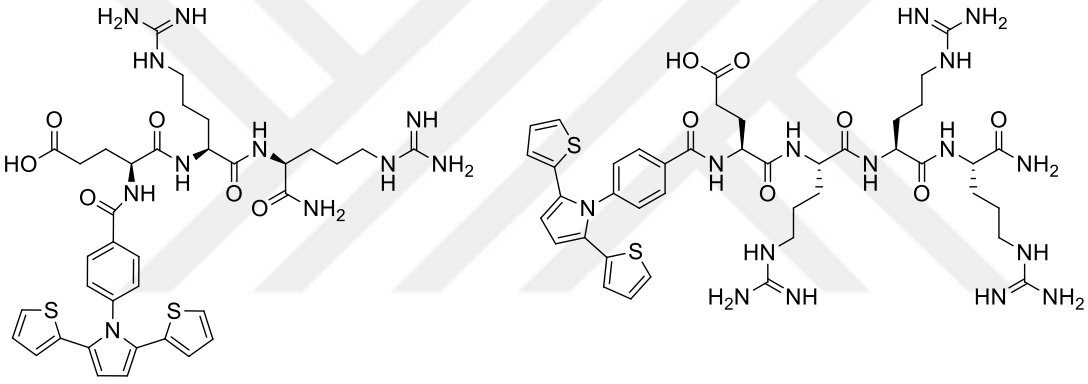

17 **18**

Figure 1.10. SNS-ERR and SNS-ERRR molecules for glucose detection[34].

CHAPTER 2

RESULTS AND DISCUSSION

2.1. Synthesis of 9,10-bis(aminomethyl)anthracene

9,10-bis(aminomethy)anthracene was synthesized based on the literature procedure starting from commercially available anthracene [35].

In the first step of the synthesis, bromomethylation reaction of anthracene was performed with paraformaldehyde and HBr in acetic acid to obtain compound **21** in 70% yield [35]. In the second step, 9,10-bis(bromomethyl)anthracene with hexamethylenetetramine (HMTA) led to the formation of compound **22** which is described as Deléphine reaction in 56% yield. ^{1}H NMR data of compound **22** is consistent with literature [35]. Overall synthesis of 9,10-bis(aminomethyl)anthracene can been seen in Scheme 2. 1.

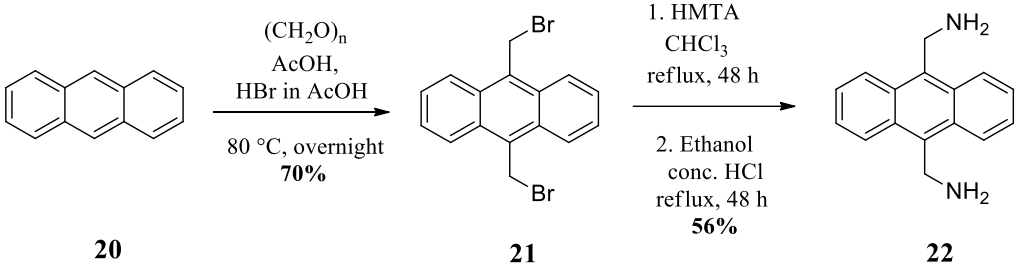

Scheme 2. 1. Overall synthesis of compound **22**.

2.2. Synthesis of 2,6-pyridinedicarboxyaldehyde

2,6-pyridinedicarboxyaldehyde was synthesized in three steps starting from commercially available 2,6-pyridinedicarboxylic acid (**23**). In the first step [36], compound **23** was treated with thionyl chloride ($SOCl_2$) and methanol to give its methyl ester derivative **24** with 99% yield (Scheme 2. 2).

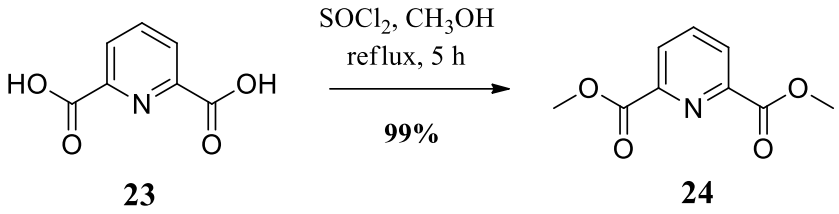

Scheme 2. 2. Synthesis of compound **24.**

Then, compound **24** was reduced to 2,6-pyridinedimethanol (**25**) by using the sodium borohydride ($NaBH_4$) and ethanol with a yield of 55% (Scheme 2. 3) [37].

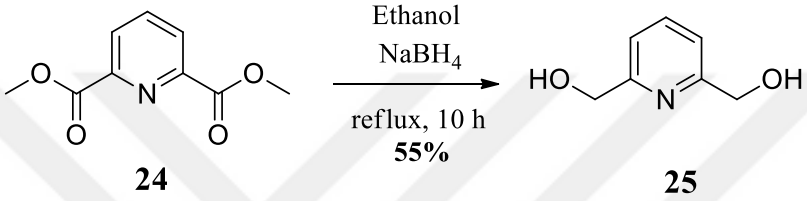

Scheme 2. 3. Synthesis of compound **25**.

The last step of the synthesis was allylic oxidation reaction with selenium dioxide (SeO_2) in 1,4-dioxane to obtain 2,6-pyridinedicarboxyaldehyde (**26**) which was purified with column chromatography in 56% yield (Scheme 2. 4). ^{1}H NMR data of compound **26** is consistent with the literature [38].

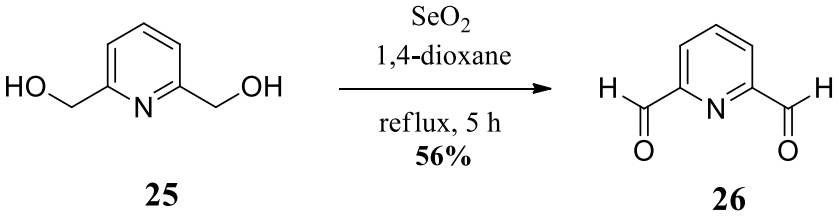

*Scheme 2. 4. Synthesis of compound **26.***

2.3. Synthesis of Anthracene-Based Macrocycle

After synthesis and purification of 2,6-dicarboxyaldehyde (**26**) and 9,10-bis(aminomethyl)anthracene (**22**), compound **14** was synthesized in two steps according to the literature procedure [26].

In the first step of the synthesis, **24** and **20** were mixed to form cyclic tetraimine derivative **25** with the yield of 40% (Scheme 2. 5).

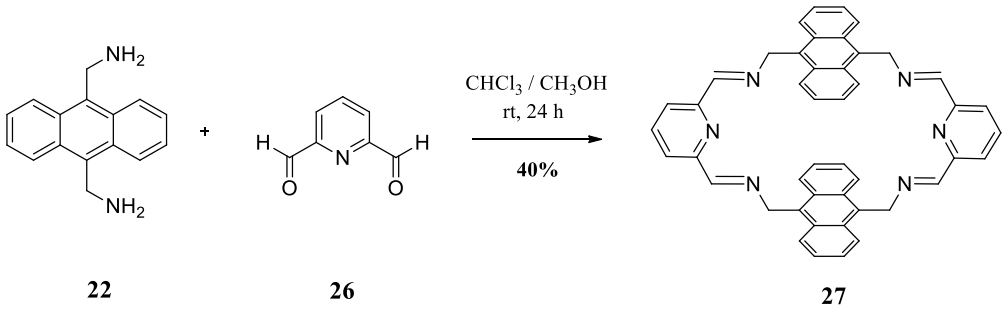

Scheme 2. 5. Synthesis of compound **27**.

Several methods were attempted to reduce compound **27** with $NaBH_4$. However, no desired product was obtained. Therefore, reduction reaction with lithium aluminum hydride ($LiAlH_4$) was applied in dry THF to obtain **MC-1** (Scheme 2. 6) [39]. Then, **MC-1** was precipitated as HCl salt in hydrogen chloride solution, 4.0 M in 1,4-dioxane. The precipitate was dissolved in water with 0.1% TFA and the reverse phase HPLC was performed for purification in low yield (30%). After purification of **MC-1**, HPLC chromatogram (Figure 2.1) of sample was recorded by using RP-C18 analytical column. Desired molecule MC-1 was characterized by ^{1}H, ^{13}C NMR and HRMS.

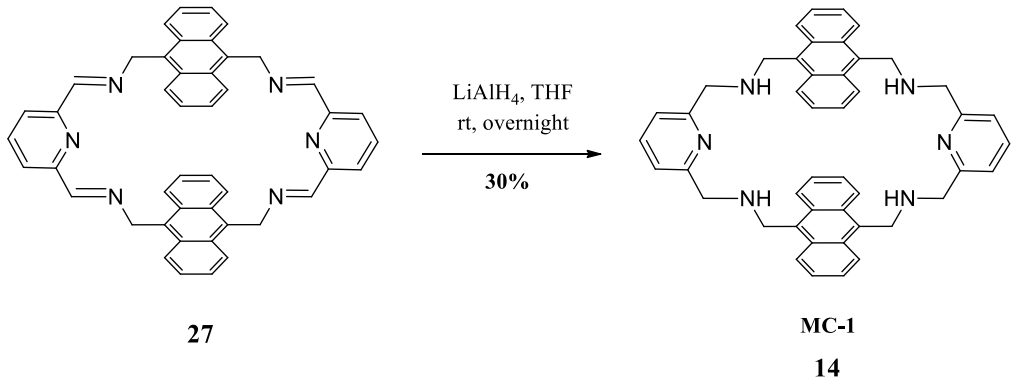

Scheme 2. 6. Synthesis of **MC-1.**

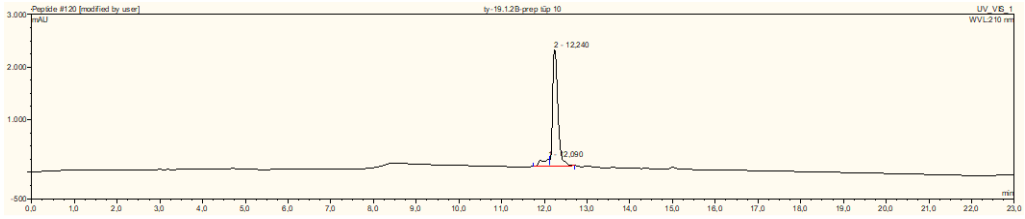

Figure 2.1. HPLC chromatogram of purified **MC-1** (compound **14**). Absorbance was monitored at 210 nm.

2.4. Sensor Studies

After **MC-1** was successfully obtained, the sensor studies were performed by Fluoresence Spectrometer by following procedures known in the literature [30]. Stock solution of **MC-1** and various aromatic compounds, namely, Picric Acid (PA), 2,4-Dinitrophenol (2,4-DNP), 4-Nitrophenol (4-NP), 2,4,6-Trinitrotoluene (2,4,6-TNT), Nitrobenzene (NB), Benzoic Acid (BA), and Phenol were prepared in THF:HEPES (9.5:0.5) at concentrations of $1.0x10^{-5}$ M. The fluorescence and absorbance of **MC-1** with different analytes was performed the subsequent addition of the compounds in 10^{-5} M buffer solution (pH = 7.2) in a quartz cuvette (1 cm x 1 cm). After sequential addition at room temperature, the mixtures of the analytes were recorded to obtain the fluorescence and absorbance spectra. The fluorescence intensity was decreased, when the fluorescence titration experiments of **MC-1** carried out with different aromatic compounds as shown in Figure 2.2.

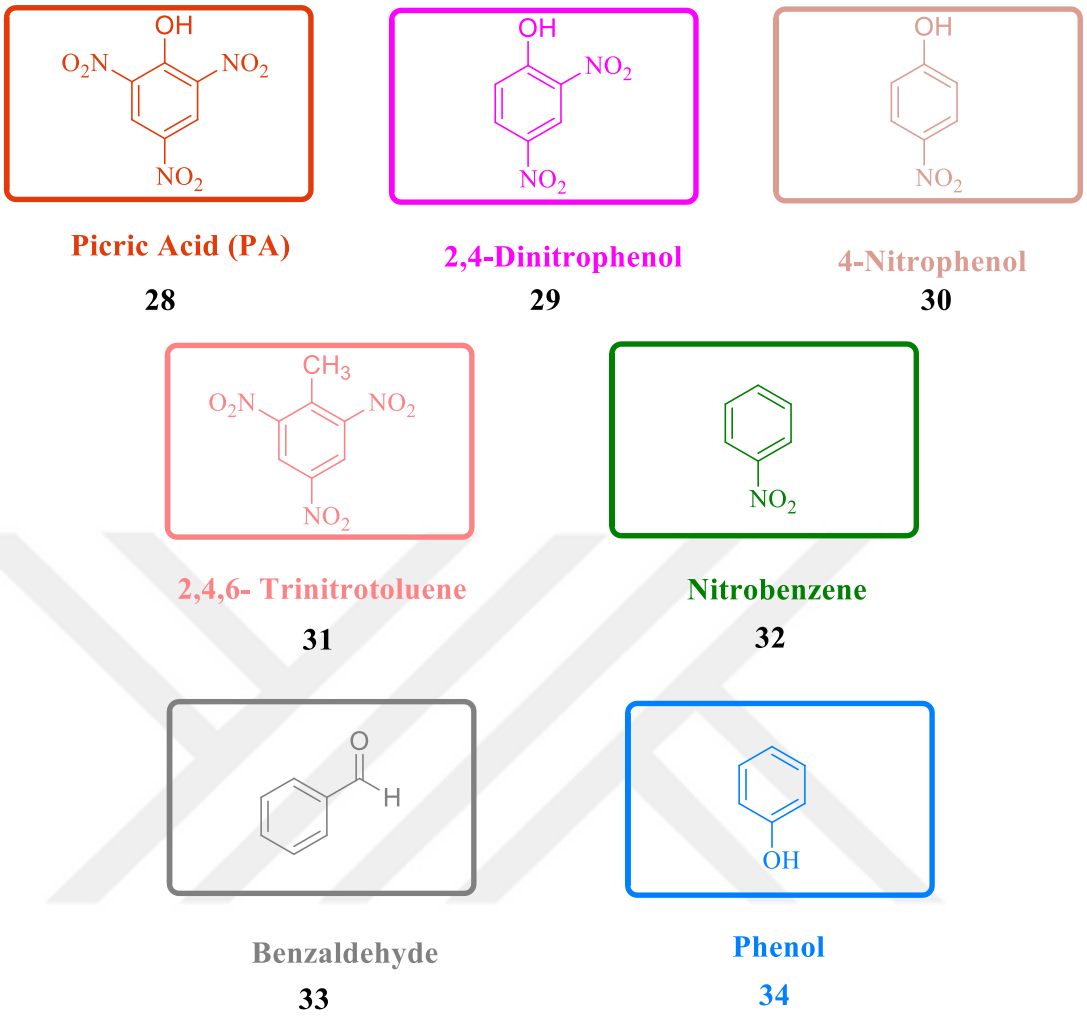

Figure 2.2. Different aromatic compounds that were used in fluorescence titration experiments.

Upon the addition of 4-Nitrophenol (4-NP), 2,4,6-Trinitrotoluene (2,4,6-TNT), Nitrobenzene (NB), Benzoic Acid (BA), and Phenol there wasn't significant change in fluorescence of the **MC-1**. However, fluorescence intensity decreased upon addition of picric acid (PA) and 2,4-Dinitrophenol (2,4-DNP) to result in fluorescence quenching. Fluorescence spectra of **MC-1** with c = 1.0 x10^{-5} M in the absence and presence of PA, and 2,4-DNP as 1:1 concentration ratio was shown in Figure 2.3 (A), and percentage change of fluorescence intensity which was calculated by using the equation % = (1-I/I_o) x 100% where I_o is the fluorescence intensity in the absence of analyte, and I is the fluorescence intensity in the presence of analyte, as 1:100

concentration ratio with different aromatic compounds was illustrated in Figure 2.3 (B).

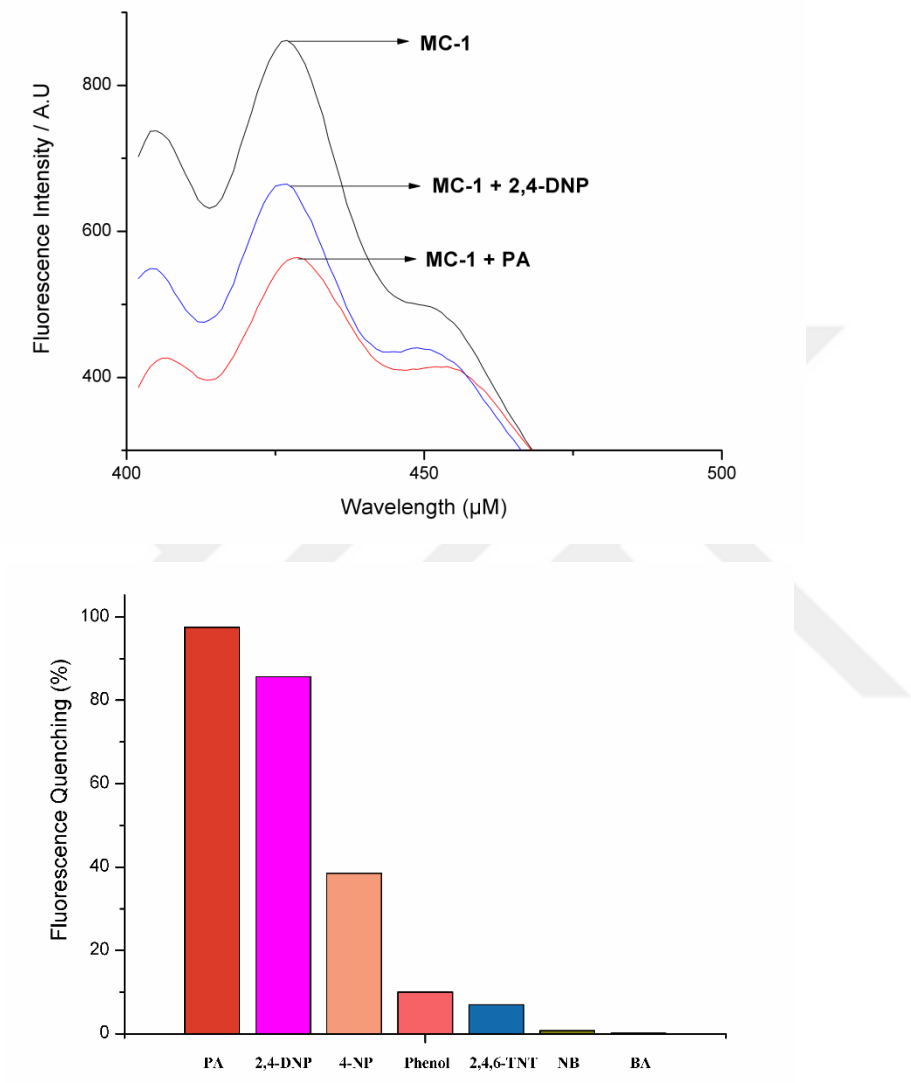

Figure 2.3. (A) Fluorescence spectra of **MC-1** with c =10-5 M upon the addition of different aromatic compounds (1:1). (B) Relative fluorescence intensity of **MC-1** with different aromatic compounds (1:100).

To examine the selectivity of **MC-1** towards PA and 2,4-DNP, the fluorescence titration experiments with different amount of these analytes starting from 0 μM to

120 μM were performed. Figure 2.4 demonstrated that the fluorescence intensities slowly decreased upon addition of increasing amount of PA and 2,4-DNP.

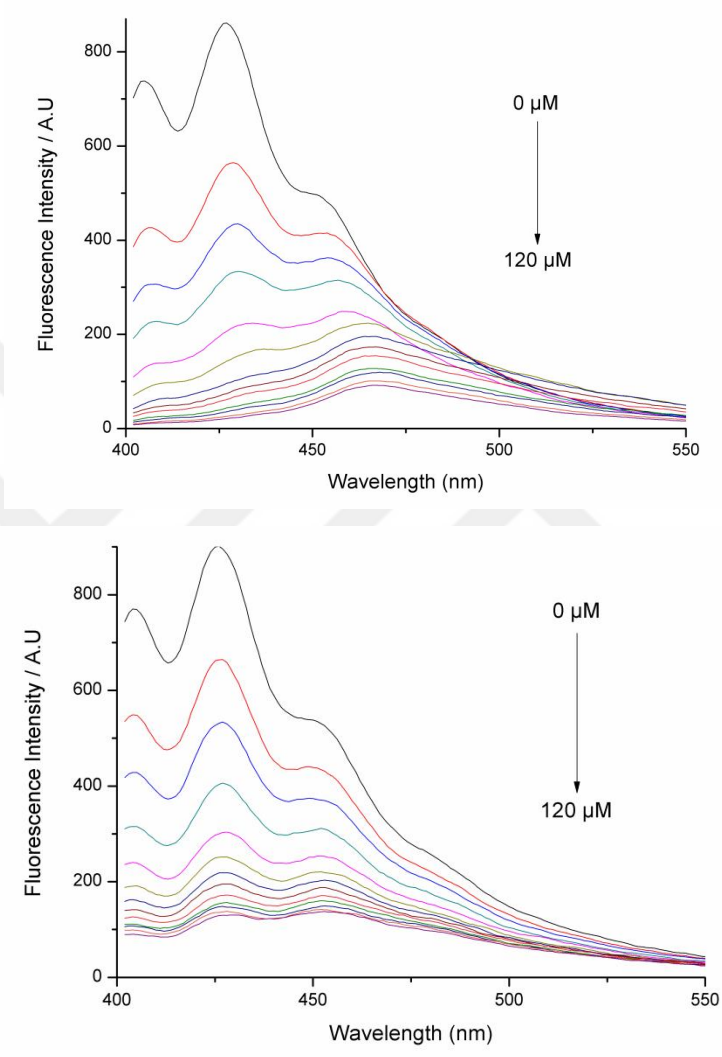

Figure 2.4. Fluorescence change of **MC-1** (1.0x10-5) with different amount of PA and 2,4-DNP in THF:HEPES (9.5:0.5).

UV-Vis study was carried to learn more information about the interaction between **MC-1** and PA. Absorption spectra of **MC-1** exhibited maximum absorbance around 380 nm. Upon addition of PA from 0 μM to 120 μM, a new shoulder like peak

appeared at 430 nm (at 120 µM PA concentration). This subsequent increase in absorbance band referred that ground state complex was formed with PA (Figure 2.5).

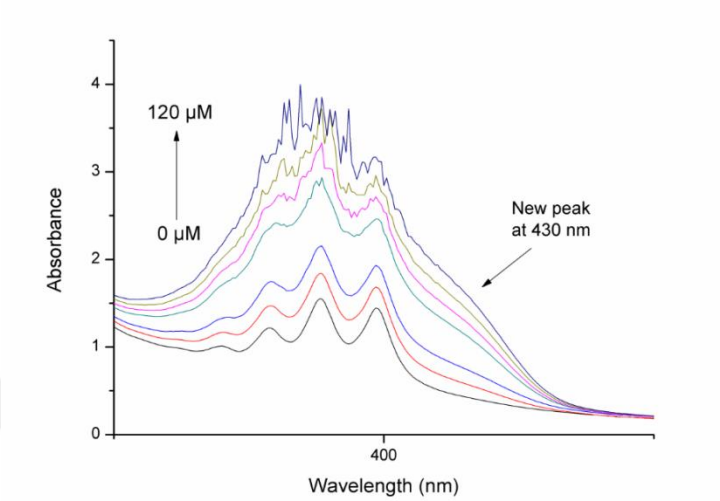

Figure 2.5. UV-Vis absorption spectra of **MC-1** (10-5 M) with increasing amount of PA.

Fluorescence titration curve was used to determine detection limit (DL). Calculation of detection limit was performed by using the equation DL = 3σ/K, where σ is the standart deviation (SD) for **MC-1** without PA in buffer solution, and K expresses the slope of the curve. DL was found to be 0.39 µM for PA and 0.25 µM for 2,4-DNP.

To identify the type of quenching behaviour, Stern-Volmer constant was calculated for PA and also 2,4-DNP using the following equation 1:

$$\frac{F_0}{F} = 1 + Ksv[Q] \qquad \text{(Equation 1)}$$

In this equation, where F_0 and F are fluorescence intensities of **MC-1** in the absence and the presence of the quencher, K_{sv} is the Stern-Volmer quenching constant, and Q is the molar concentration of quencher. By using this equation, Stern-Volmer constant was calculated. According to the slope of the Stern-Volmer plot, It was found to be 5.28×10^4 M^{-1} for PA (Figure 2.6 (A)) and 5.61×10^4 M^{-1} for 2,4-DNP (Figure 2.6 (B)).

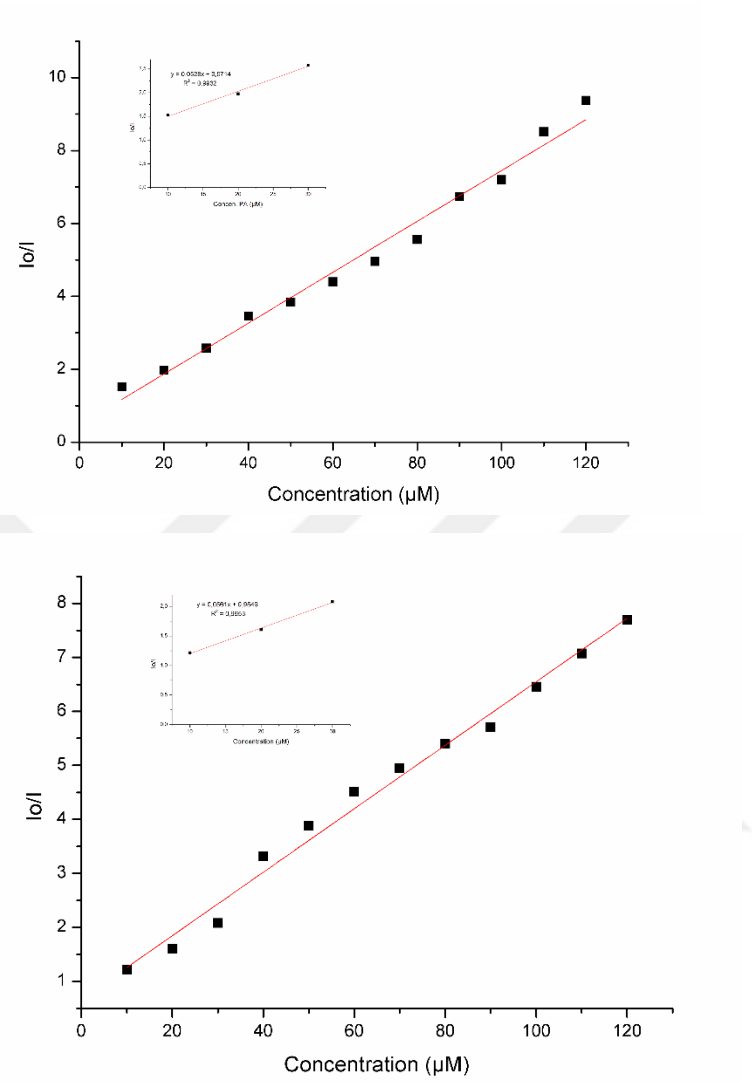

Figure 2.6. Stern-Volmer plot of **MC-1** (a) for PA (b) for 2,4-DNP.

Determination of binding stoichiometry and binding constant were performed by drawing Benesi-Hildebrand plot as defined in literature [40]. Following the Benesi-Hildebrand equation (Equation 2), association constant K_a was calculated. In this equation F_0 is fluorescence intensity of **MC-1**, F is the fluorescence intensity of **MC-1** with PA, F_{min} is the fluorescence intensity of **MC-1** in maximum amount of PA and, [PA] is the concentration of picric acid.

$$\frac{1}{(F_0-F)} = \frac{1}{\{Ka(Fo-Fmin)[PA]\}} + \frac{1}{(Fo-Fmin)} \qquad \text{(Equation 2)}$$

Association constant could be calculated from the Benesi-Hildebrand plot between $1/(F_0\text{-}F)$ against 1/[PA]. The association constant for **MC-1** with PA was found to be $K_a=1.01x10^4\ M^{-1}$. In Figure 2.7, the linearty of Bensei-Hildebrand plot indicated the 1:1 stoichiometry between **MC-1** and PA.

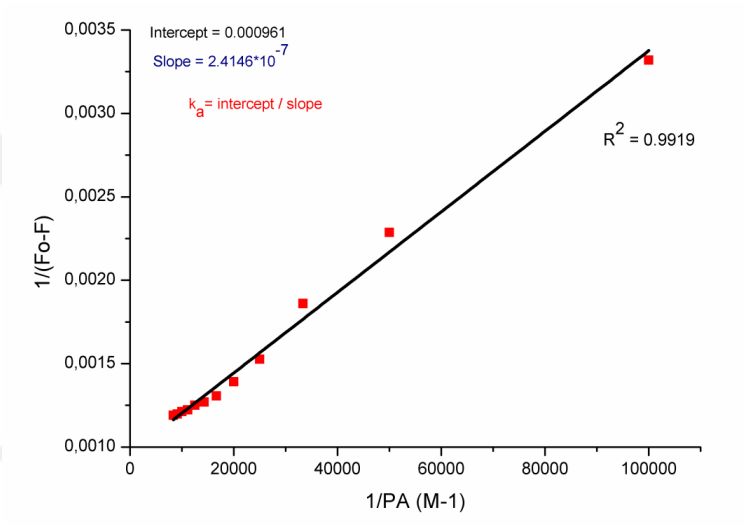

Figure 2.7. The Benesi-Hildebrand plot of **MC-1** with PA.

The comparison of quenching constant, K_{sv}, detection limit, and media used for picric acid detection with some recent reports in literature are summarized in Table 2.1.

Table 2.1. *The comparison of Ksv, detection limit, and media used for PA detection.*

Publication	Material Used	K_{sv} (M^{-1})	Detection Limit	Media
Our Work	Anthracene-based macrocycle	5.3×10^4	0.39 µM	THF : HEPES (v/v=9.5:0.5)
Chem.Commun. 2012, 48, 5007.	Fluoranthene derivative	9.9×10^4	0.087 µM	Ethanol
Appl. Mater. Interfaces, 2009, 7, 1379.	Phosphole oxide	2.0×10^4	2.0×10^3 µM	10% THF in water
Chemistry Select, 2016, 1, 1756-1762.	Benzimidazolium salt	1.6×10^4	0.21 µM	H_2O
Chem. Mater. 2014, 26, 4221.	Graphene derivative	8.9×10^5	1.3 µM	H_2O/THF (v/v=9:1)
Chem. Mater. 2014, 26, 4221.	Graphene derivative	8.9×10^5	1.3 µM	H_2O/THF (v/v=9:1)
ACS Appl. Mater. Interfaces, 2013, 5, 5373.	Hexa-peri-hexabenzocoronene Derivative	3.2×10^6 & 2.0×10^6	0.004 µM & 0.009 µM	H_2O/THF (v/v=4:6)
International Journal of Spectroscopy, 2018, 1-5.	Anthracene derivative	1.8×10^7	2.8 µM	THF/HEPES (v/v=9.5:0.5)

2.5. Synthesis of SNS molecule

2.5.1. Synthesis of methyl-4-aminobenzoate

Methyl 4-aminobenzoate was synthesized starting from 4-aminobenzoic acid. Compound **35** was treated with thionyl chloride in methanol to give compound **36** with the yield of 88% (Scheme 2. 7). ^{1}H NMR data of compound **36** is consistent with the literature [41].

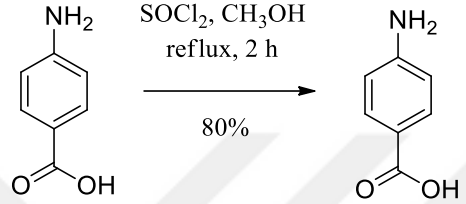

35 **36**

Scheme 2. 7. Synthesis of compound **36**.

2.5.2. Synthesis of 1,4-dithiophene-2-yl-butane-1,4-dione

Compound **39** was synthesized by Friedel-Crafts acylation reaction with thiophene and succinyl chloride using $AlCl_3$ with the yield of 48% [42] (Scheme 2. 8).

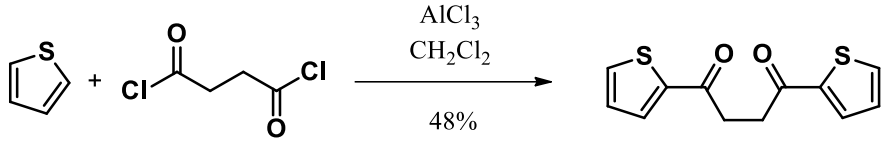

37 **38** **39**

Scheme 2. 8. Synthesis of compound **39**.

2.5.3. Synthesis of methyl 4-(2,5-di(thiophen-2-yl)-1H-pyrrol-1-yl) benzoate

Methyl-4-aminobenzoate with pTSA as a catalyst in toluene was refluxed under argon to give compound **40** with 61% yield (Scheme 2. 9) which is describes as Paal-Knorr pyrrole synthesis [43].

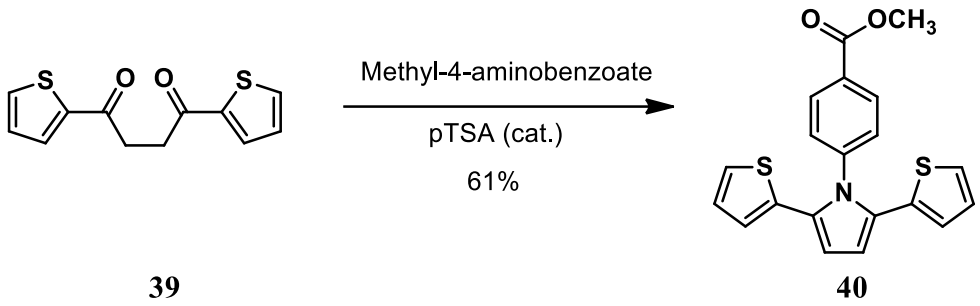

39 **40**

Scheme 2. 9. Synthesis of compound **40**.

2.5.4. Synthesis of methyl 4-(2,5-di(thiophen-2-yl)-1H-pyrrol-1-yl) benzoic acid

Compound **40** was hydrolyzed with LiOH in a THF/MeOH mixture at room temperature to give SNS-COOH monomer (**41)** with yield of 88% [4] (Scheme 2. 10) [44].

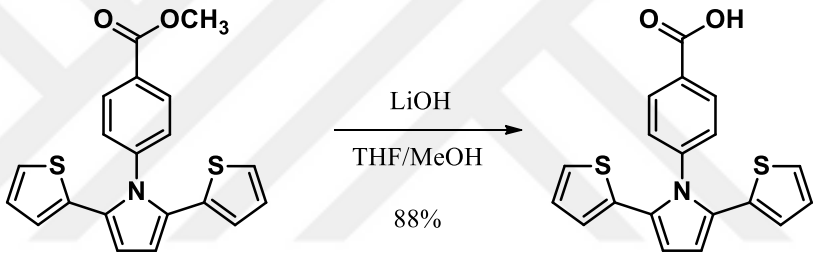

40 **41**

Scheme 2. 10. Synthesis of compound **41**.

2.6. Synthesis of SNS-ERR and SNS-ERRR

Compound **17** and compound **18** was synthesized by solid phase peptide synthesis. Coupling was performed by using ring amide resin (0.05 mmol) under microwave conditions (at 20 W) at 75 ℃ with HBTU in DMF as the coupling agent and DIEA as the base. 5.5 fold amino acids were coupled for 5 minutes. After this coupling reaction, deprotection of Fmoc groups was done by using 20% piperidine solution in DMF solution (Scheme 2.11)

SNS-peptide conjugation was performed on resin by using the same coupling conditions for the amino acids. 95% TFA-2.5% TIPS-2.5% H_2O solution was used to

remove the side chain protecting groups on amino acids and cleave the peptide derivatives from the resin. The crude SNS-COOH monomer conjugated peptide derivatives (compound **17** and compound **18**) were purified by semi- preparative RP-HPLC. LC-MS and 1H NMR spectroscopy were applied to confirm the structures.

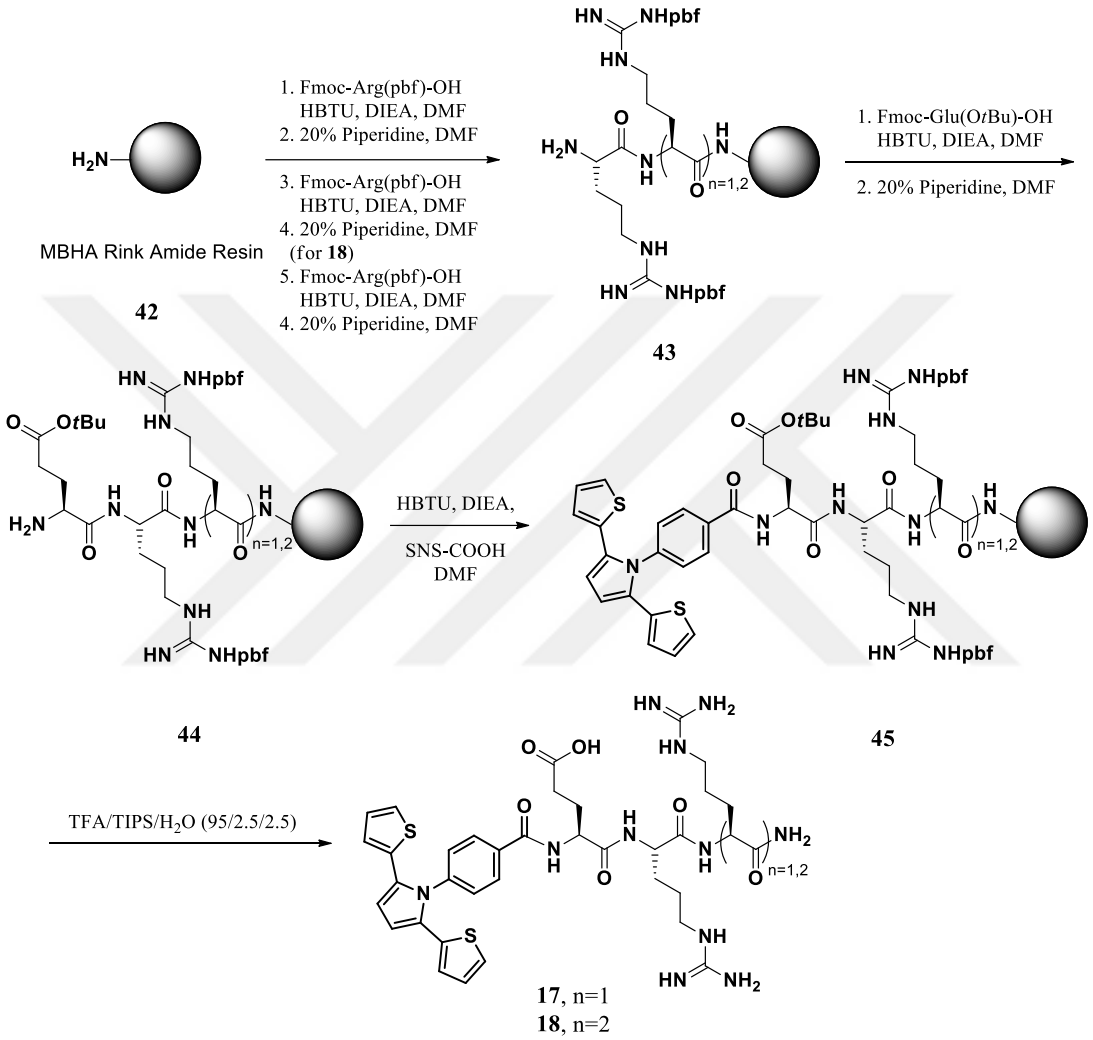

Scheme 2. 11. Synthesis of SNS-ERR and SNS-ERRR conjugated peptides by using solid phase peptide synthesis.

2.7. Conclusion

2.7.1. Explosive detection

In this study, we synthesized anthracene-based macrocycle **MC-1**. The sensor application of **MC-1** was examined on addition of different aromatic compounds using Fluorescence Spectrometer. Fluorescence intensity was influenced a lot with the increasing amount of PA and 2,4-DNP to result in fluorescence quenching. Stern-Volmer constants were determined from the slope of the Stern-Volmer plot. In general, sensitive sensor systems have steeper Stern-Volmer slope, as a consequence, the Stern-Volmer constant becomes higher. The quenching constans were found to be $5.28x10^4$ M^{-1} for PA and $5.61x10^4$ M^{-1} for 2,4-DNP. The high K_{sv} values indicate the sensitivity of the **MC-1** to PA and 2,4-DNP as a quencher. Detection limit is described as the lowest amount or concentration of a desired compound that can be detected with designed method or molecule. The detection limits were calculated with the equation DL = 3σ/K, and they were found to be 0.39 μM for PA and 0.25 μM for 2,4-DNP. These values demonstrated that **MC-1** was a good example of anthracene-based macrocycle for selective sensing of PA.

High value of association constant, $K_a=1.01x10^4$ M^{-1}, and the 1:1 binding stoichiometry expressed that strong complex formation occurred between **MC-1** and PA.

2.7.2. Glucose detection

In this study, water-soluble SNS-ERR and SNS-ERRR were synthesized via solid phase peptide synthesis. Monomers were characterized by using ^1H, ^{13}C NMR and FTIR and HRMS. RP-HPLC was used to purify monomers. Polymerization and application of SNS-ERR and SNS-ERRR monomers were performed by Toppare research group. The results were found a linear range of 0.01-0.75 $mmolL^{-1}$ ($R^2=0.998$), a sensitivity of 91.37 μA $mM^{-1}cm^{-2}$, and K_m^{app} value of 0.208 $mmolL^{-1}$. These results indicate that SNS-type conjugated polymer exhibit selective and sensitive detection of glucose molecule.

CHAPTER 3

EXPERIMENTAL

3.1. Materials and Methods

Anthracene was supplied from Riedel-De Haen, Hannover.

2,6-pyridinedicarboxylicacid was supplied from Sigma Aldrich, Germany.

HPLC grade solvents were supplied from Sigma Aldrich, Germany.

Other solvents are technical grade. They were purified, when necessary, using distillation method.

Nuclear magnetic spectra were read in $CDCl_3$ and CD_3OD on Bruker Spectrospin Advance DPX 400 spectrometer. Chemical shifts were received in parts per million (ppm) with TMS as internal reference. NMR spectra of the compounds are given in Appendix A.

HPLC chromatogram was read on an Agilent 1100 Series. HPLC chromatograms of compounds are given in Figure 10.

The mass spectra were recorded on Agilient 7890 A 5975C VL MSD GC/MS.

3.2. Synthesis of 9,10-bis(bromomethyl)anthracene

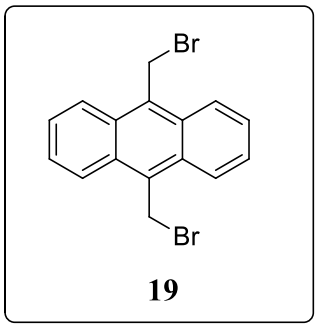

19

Based on the literature [32], to a solution of anthracene (2.50 g, 14.0 mmol) and paraformaldehyde (0.840 g, 28.0 mmol) in acetic acid (10 mL) was stirred at room temperature. HBr in acetic acid (33% wt, 13.75 mL) was added drop by drop over 1 hour. Then the reaction temperature was warmed to 80 °C. After mixture was cooled to room temperature, the yellow precipitate was collected on a filter and washed with water. The crude product was recrystallized from toluene to obtain 9,10-bis(bromomethyl)anthracene with 70% yield.

^{1}H NMR ($CDCl_3$, 400 MHz): δ (ppm) 8.31 (m, *J* = 6.8, 3.2 Hz, 4H), 7.61 (m, *J* = 6.9, 3.2 Hz, 4H), 5.45 (s, 4H).

3.3. Synthesis of 9,10-bis(aminomethyl)anthracene

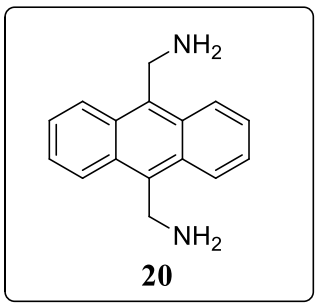

20

Based on the literature procedure [32], 9,10-bis(bromomethyl)anthracene (1.0 g, 2.7 mmol) was suspended in chloroform (150 mL), and hexamethylenetetraamine (1.0 g, 7.1 mmol) was added to the mixture. Then reaction was refluxed for 48 hours. The mixture was warmed to room temperature, and precipitate was collected on a filter.

After air-drying, the yellow solid was suspended in ethanol (130 mL) and concentrated HCl aq. (25 mL) was added to the mixture. Then, the reaction was refluxed 48 hours. After cooling to 0 °C the resulting precipitate was filtered and washed with cold ethanol. The solid was suspended in Na_2CO_3 aq. (2.0 M, 250 mL) to neutralize the resulting amine, while stirring at room temperature. The mixture was extracted with chloroform (150 mL). After addition of extra chloroform (100 mL), the organic phase was separated from aqueous phase and dried over $MgSO_4$. The solvent was evaporated with using rotary evaporator to obtain yellow solid in the yield of 56%.

^{1}H NMR ($CDCl_3$, 400 MHz): δ (ppm) 8.34 (m, *J* = 6.9, 3.2 Hz, 4H), 7.50 (m, *J* = 6.9, 3.2 Hz, 4H), 4.77 (s, 4H), 1.56 (s, 1H).

3.4. Synthesis of dimethyl 2,6-pyridinedicarboxylate

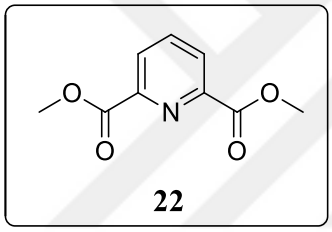

22

Based on the following literature [33], 2,6-pyridinedicarboxylic acid (1.0 g, 5.98 mmol) was dissolved in methanol (30 mL). Then, thionyl chloride (30 mL) was added slowly to a solution while stirring and cooling in an ice bath. The reaction was refluxed for 5 hours. After solvent was evaporated/removed, the residue was diluted with saturated $NaHCO_3$ aq. and extracted with DCM (45 mL). The organic phases were combined/joined together and dried with Na_2SO_4. After filtration, the solvent was evaporated to obtain white crystalline powder in 97% yield.

^{1}H NMR ($CDCl_3$, 400 MHz): δ (ppm) 8.28 – 8.24 (d, 2H), 7.96 (t, *J* = 7.8, 4.1 Hz, 1H), 3.96 (s, 6H).

3.5. Synthesis of 2,6-pyridinedimethanol

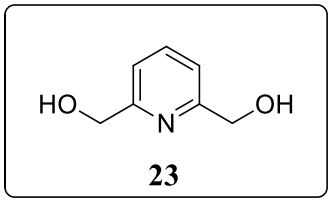

23

Based on the literature [34.], stirring solution of dimethyl 2,6-pyridinedicarboxylate (0.867 g, 4.44 mmol) in ethanol (3.55 mL) was added $NaBH_4$ (0.672 g, 17.9 mmol) slowly in an ice bath. Then, the mixture was stirred at 0 °C for 1 hour. After removal of an ice bath, the mixture was stirred at room temperature another 2 hours. The reaction was allowed to heat at reflux on a steam bath for 10 hours. The solvent was evaporated, and acetone (3.5 mL) was added to the residue. The mixture was refluxed for 1 hour. After the solvent was removed, aqueous solution of K_2CO_3 (3.5 mL) was added and refluxed for 1 hour. Then, water was added (10 mL). The mixture was continuously extracted with chloroform to obtain the white powder with yield of 55%.

^{1}H NMR (DMSO, 400 MHz): δ (ppm) 7.78 (t, *J* = 7.7 Hz, 1H), 7.31 (d, *J* = 7.7 Hz, 2H), 5.39 (t, *J* = 5.7 Hz, 2H), 4.52 (d, *J* = 5.6 Hz, 4H).

3.6. Synthesis of 2,6-pyridinedicarboxyaldehyde

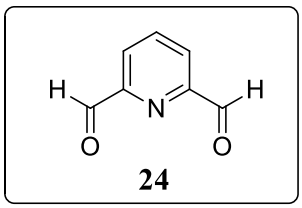

24

Based on the literature [35], SeO_2 (0.118 g, 1.06 mmol) was added to a dioxane (3.0 mL) solution of 2,6-pyridinedimethanol (0.148 g, 1.06 mmol). Then, the reaction mixture was refluxed while stirring for 5 hours. The vacuum filtration was applied to separate oxide residue from the solution. Then, the brownish filtrate was evaporated by using rotary evaporator. The solid was purified with flash column chromatography (EtOAc:Hexane = 1:3) on silica gel to give pale yellow solid. Yield is 56%.

^{1}H NMR ($CDCl_3$, 400 MHz): δ (ppm) 10.11 (s, 2H), 8.14 – 8.08 (d, *J*= 7.3, 2H), 8.02 (t, *J* = 7.9, 1H).

3.7. Synthesis of 3,7,11,15-tetraaza-1,9(2,6)-dipyridina-5,13(9,10)-dianthracenacyclohexadecaphane (14)

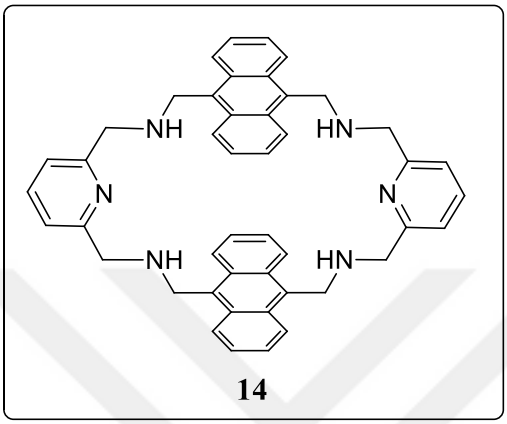

14

Based on the following literature [26], 9,10-bis(aminomethyl)anthracene (0.500 mmol, 118 mg) was dissolved in 40 ml of methanol. Then 2,6-pyridinedicarboxyaldehyde (0.500 mmol, 67.5 mg) in a mixture of methanol and chloroform (20 mL of each solvent) was added drop by drop to a stirring solution. After 24 hours stirring at room temperature, the yellow solid was filtrated and washed with methanol several times. The solid was allowed to dry. Without purification, the yellow solid (0.15 mmol, 100 mg) was dissolved in a dry THF (17 mL). $LiAlH_4$ (0.09 g) was added slowly over 2 hours. Then the mixture was stirred 24 hours. 8.0 mL of water, 8.0 mL of NaOH (15%), and 20 mL of water were added. The yellow solid was filtrated, washed with H_2O and extracted with chloroform [36]. The yield was 30%.

^{1}H NMR (D_2O, 400 MHz): δ 7.84 – 7.77 (m, 4H), 7.68 – 7.56 (m, 8H), 7.45 – 7.35 (m, 10H) (16 aliphatic hydrogens are below solvent peak between 4.5 and 5.0 ppm).

^{13}C NMR (D_2O, 100 MHz): 42.49, 49.62, 123.20, 214.29, 127.98, 130.37, 140.33, 151.67.

HRMS $C_{46}H_{42}N_6$ $[M\text{-}Na]^+$: Calculated 701. 3369, found 701.3330.

3.8. Synthesis of 4-amino-methyl-benzoate

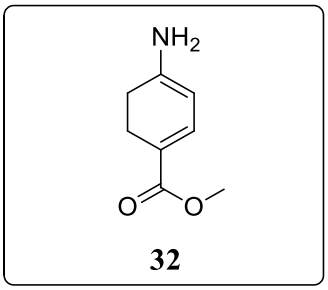

32

Based on the following literature [41], 4-aminobenzoic acid (0.70 g, 5.2 mmol) was dissolved in methanol (15 mL). Thionyl chloride (2.95 mL, 41.1 mmol) was added dropwise under N_2 at 0 °C. After mixture was stirred at room temperature, then refluxed for 2 hours. After reaction was completed, saturated Na_2CO_3 was added. The mixture was extracted with ethyl acetate. The yield was 80%.

^{1}H NMR ($CDCl_3$, 400 MHz): δ 7.86-7.68 (d, *J*= 8.66, 4H), 6.63-6.52 (d, *J*= 8.66, 4H), 3.99 (s, 2H), 3.78 (s, 3H).

3.9. Synthesis of 1,4-dithiophene-2-yl-butane-1,4-dione

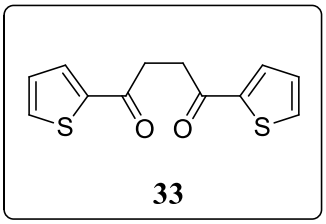

33

Based on the following literature [42], a solution of thiophene (4.08 mL, 0.06 mol) and $AlCl_3$ (8.0 g, 0.06 mol) in dry CH_2Cl_2 (25.0 mL) was added dropwise to a suspension of succinyl chloride (2.75 mL, 0.025 mol) in dry CH_2Cl_2 (25 mL) at 0 °C. The mixture was stirred at 18-20 °C for 4 h and poured into a mixture of 50 g ice and 5 mL HCl, and stirred for 1 hour and the resulting dark green organic phase was washed with concentrated $NaHCO_3$, and dried over Na_2SO_4. After the solvent was evaporated, a blue-green solid remained and is suspended in ethanol. The yield was 48%.

^{1}H NMR ($CDCl_3$, 400 MHz): δ 7.76 (d, *J*= 3.74, 2H), 7.59 (d, *J*= 4.93, 2H), 7.07 (t, *J*=4.29-4.17, 2H), 3.46 (s, 4H).

3.10. Synthesis of methyl 4-(2,5-di(thiophen-2-yl)-1H-pyrrol-1-yl) benzoate

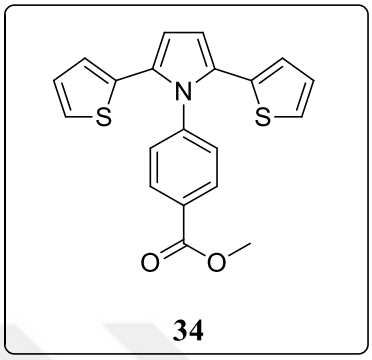

34

Based on the following literature [43], a round-bottomed flask equipped with an argon inlet and mechanical stirrer was charged with 1,4-di(2-thienyl)-1,4-butanedione (0.625 g, 2.0 mmol), methyl-4-aminobenzoate (2.5 mmol,), PTSA (43.75 mg, 0.23 mmol) as catalyst and 7.5 mL toluene. The mixture was stirred and refluxed for 24 h under argon. Evaporation of the toluene was followed by chromatography with CH_2Cl_2. The yield was 61%.

^{1}H NMR ($CDCl_3$, 400 MHz): δ 7.79 (d, *J*= 8.46, 2H), 7.29 (d, *J*=8.44, 2H), 7.02 (d, *J*= 5.1, 2H), 6.72 (t, *J*= 3.78-4.95, 2H), 6.51 (s, 2H), 6.42 (d, *J*= 3.52, 2H), 3.87 (s, 3H).

3.11. Synthesis of methyl 4-(2,5-di(thiophen-2-yl)-1H-pyrrol-1-yl) benzoic acid

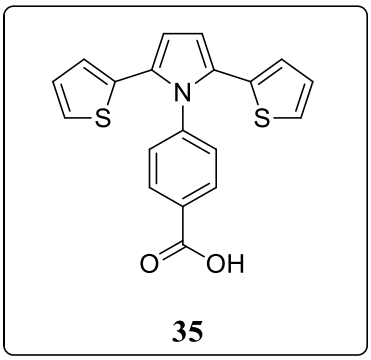

35

Based on the following literature [44], methyl 4-(2,5-di(thiophen-2-yl)-1H-pyrrol-1-yl) benzoate (0.281 g, 0.801 mmol) was dissolved in CH_3OH/THF (2:1, 15 mL) and mixed with $LiOH.H_2O$ (20 mmol, 10 mL) and the reaction mixture was stirred for 2 h at room temperature. The mixture was neutralized by HCl (6 M, pH: 2-3) prior to removing the CH_3OH/THF by evaporation under reduced pressure. The suspension was dissolved in DCM followed by washing with water (15 mL) and brine (15 mL), then dried over Na_2SO_4, evaporated to dryness under reduced pressure. The yield was 88%.

^1H NMR ($CDCl_3$, 400 MHz): δ (ppm) 8.01 (d, J= 8.46, 2H), 7.52 (d, J= 8.46, 2H), 7.36 (d, J= 5.08, 2H), 6.92 (t, J= 3.62-5.13, 2H), 6.72 (d, J= 3.56, 2H), 6.61 (s, 2H).

3.12. Synthesis of SNS-ERR

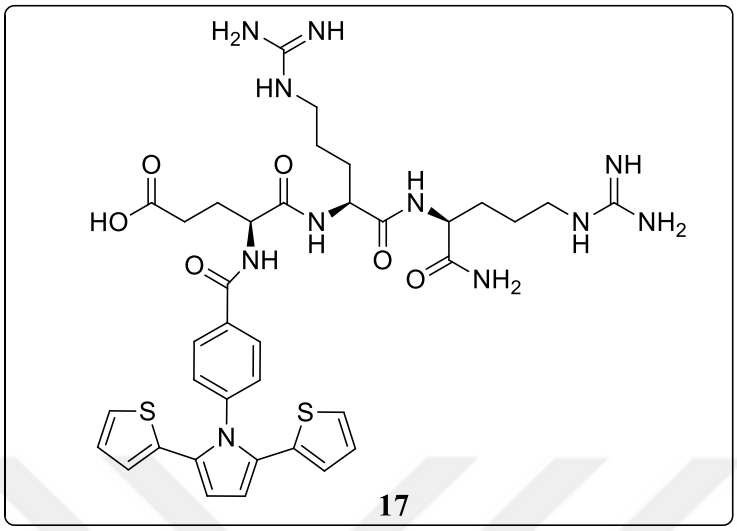

17

Based on the general procedure of solid phase peptide synthesis, compound **17** was synthesized starting with 0.05 mmol ring amide resin. 356 mg (0.55 mmol) of Fmc-Arg (Pbf), 234 mg (0.55 mmol) of Fmoc-Glu (OtBu) and 105 mg (0.3 mmol) SNS-COOH were used to obtain compound **17.**

^{1}H NMR (DMSO, 400 MHz): δ (ppm) 8.92 (d, J = 6.7 Hz, 1H, −NH−CH), 8.45 (d, J = 6.7 Hz, 1H, −NH−CH), 8.06 (d, J = 8.2 Hz, 2H), 7.42 (d, J = 8.4 Hz, 2H), 7.31 (dd, J = 5.0, 1.2 Hz, 2H), 7.16 (bs, 2H, −NH2), 6.97 (bs, 2H, −NH2), 6.89 (dd, J = 5.3, 3.6 Hz, 2H), 6.66 (dd, J =3.6, 1.2 Hz, 2H), 6.59 (s, 2H), 4.45−4.52 (m, 1H, aH), 4.05−4.10 (m, 1H, CH), 3.90−3.95 (m, 1H, CH), 2.91−3.22 (m, 4H, −CH2−N), 2.30−2.36 (m, 2H, −CH2−COOH), 1.80−1.85 (m, 2H, −CH2−), 1.49−1.66 (m, 8H, −CH2−).

HRMS $C_{46}H_{42}N_6$ $[M]^+$: Calculated 947. 4007, found 947.4018.

IR (υ) : 3306, 3188, 3500−3000 (bs), 1647, 1532, 1501, 1414, 1180, 1045, 857, 699 cm^{-1}.

3.13. Synthesis of SNS-ERRR

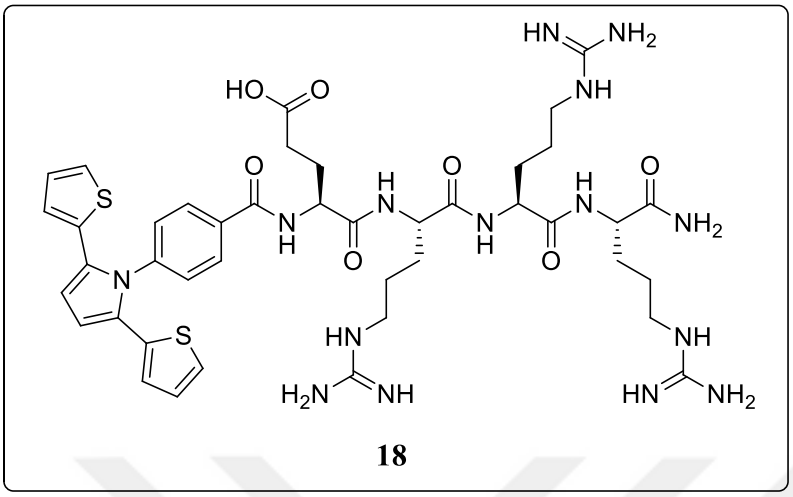

18

Based on the general procedure of solid phase peptide synthesis, compound **18** was synthesized starting with 0.05 mmol ring amide resin. 356 mg (0.55 mmol) of Fmc-Arg (Pbf), 234 mg (0.55 mmol) of Fmoc-Glu (OtBu) and 105 mg (0.3 mmol) SNS-COOH were used to obtain compound **18.**

^{1}H NMR (DMSO, 400 MHz): δ (ppm) 8.72 (d, J = 7.2 Hz, 1H, –NH–CH), 8.22 (d, J= 7.7 Hz, 1H, –NH–CH), 8.05 (d, J = 7.5 Hz, 1H, –NH–CH), 7.99 (d, J = 8.4 Hz, 2H), 7.93 (d, J = 7.7 Hz, 1H, –NH–CH),7.49 (d, J = 8.4 Hz, 2H), 7.33 (dd, J = 5.1, 1.0 Hz, 2H), 7.23 (bs, 1H, –NH), 7.13 (bs, 2H, –NH2), 7.10 (bs, 1H, –NH), 6.90 (dd, J = 5.1, 3.6 Hz, 2H), 6.68 (dd, J = 3.6, 1.1 Hz, 2H), 6.60 (s, 2H), 4.49–4.47 (m, 1H, aH), 4.24–4.30 (m, 2H, CH), 4.14–4.19 (m, 1H, CH), 3.04–3.16 (m, 6H, –CH2–N), 2.34–2.42.(m, 2H, –CH2–COOH), 1.64–1.74 (m, 2H, –CH2–), 1.46–1.58 (m, 12H, -CH_2).

IR (υ) : 3281, 3194, 3500–2950 (bs), 1647, 1533, 1501, 1414, 1170, 1042, 857, 695 cm^{-1}.

REFERENCES

1) McGhee, J. Classification of sensors. In Syedenham, P. H & Thorn, R (Eds.), *Handbook of measuring system design,* **2005**, Hoboken, New Jersey: John Wiley & Sons.

2) Hulanicki, A.; Glab, S.; Ingman, F. Chemical Sensors: Definitions and Classification. *Pure & Appl. Chem*., **1991**, *63*, 1247-1250.

3) Lakowicz, J. R. *Principles of Fluorescence Spectroscopy*. **2006,** Springer, New York.

4) Carter, K. P.; Young, A. M.; Palmer, A. E. Fluorescent sensors for measuring metal ions in living systems: a review. *Chem. Rev.*, **2011**, *114*, 4564-4601.

5) Matsuoka, Y.; Yamato, M.; Yamada, K. Fluorescence probe for the convenient and sensitive detection of ascorbic acid. *J. Clin. Biochem. Nutr.,* **2016,** *58*, 16-22.

6) Klonoff, D. C. Overview of fluorescence glucose sensing: a technology with a bright future. *J Diabetes Sci Technol,* **2012,** *6*, 1242-1250.

7) Roy, B.; Bar, A. K.; Gole, B.; Mukherjee, P. S. Fluorescent Tris-Imidazolium Sensors for Picric Acid Explosive. *J. Org. Chem.,* **2013,** *78*, 1306-1310.

8) Peng, X.; Liu, H.; Liu, Wei.; Xu, W.; Fu, Y.; He, Q.; Cao, H.; Cheng, J. Ultrasensitive and direct fluorescence detection of RDX explosive vapor via side-chain terminal functionalization of a polyfluorene probe. *Anal. Methods,* **2018,** *10*, 1695-1702.

9) Charles, P.T.; Adams, A. A.; Howell, P. B.; Trammell, S. A.; Deschamps, J. R.; Kusterbeck, A. W. Fluorescence-based sensing of 2,4,6-Trinitrotoluene (TNT) using a multi-channeled poly(methyl methacrylate) (PMMA) microimmunosensor. *Sensors,* **2010,** *10*, 876-889.

10) Heyduk, E.; Heyduk, T. Nucleic acid-based fluorescence sensors for detecting proteins. *Anal. Chem.,* **2005,** *77*, 1147-1156.

11) Dai, N.; Kool, E. T. Fluorescent DNA-based enzyme sensors. *Chem. Soc. Rev.,* **2011,** *40*, 5756-5.

12) Chen, J. W.; Chen, C. M.; Chang, C. C. A fluorescent pH probe for acidic organelles in living cells. ***Org. Biomol. Chem.,* 2017*, 15,* 7936-7943.**

13) Tsien, R. Y. New calcium indicators and buffers with high selectivity against magnesium and protons: design, synthesis, and properties of prototype structures. *Biochemistry,* **1980,** *19*, 2396-2404.

14) Grynkiewicz, G.; Poenie, M.; Tsien, R. Y. A new generation of Ca^{2+} indicators with greatly improved fluorescence properties. *J. Biol. Chem.,* **1985,** *260,* 3440-3450.

15) Minta, A.; Kao, J. P.; Tsien, R. Y. Fluorescent indicators for cytosolic calcium based on rhodamine and fluorescein chromophores. *J. Biol. Chem.,* **1989,** *264,* 8171-8180.

16) Takuya, T.; Nagano, T. Small-molecule fluorophores and fluorescent probes for bioimaging. *Pflugers Arch - Eur J Physiol,* **2013,** *465*, 347-359.

17) Czarnik, A. W. *Fluorescent Chemosensors for Ion and Molecule Recognition.* **1993,** Taylor & Francis, London.

18) Pittillo, R. F.; Woolley, C. Pseudourea, 2,2′-(9,10-Anthrylenedimethylene) bis-(2-thio-dihydrochloride) Dihydrate: Microbiological Assay and Tissue Distribution Studies in Mice. *Appl Microbil.,* **1969,** *18,* 519-521.

19) Somaskar, M. N.; Chetana, P. R. A review on anthracene and Its derivatives: applications. *RRJCHEM,* **2016,** *5,* 45-52.

20) Thangthong, A.; Meunmart, D.; Prachumrak, N.; Jungsuttiwong, S.; Keawin, T.; Sudyoadsuk, T.; Promarak, V. Synthesis and characterization of 9,10-substituted anthracene derivatives as blue light-emitting and hole-transporting materials for electroluminescent devices. *Tetrahedron,* **2012,** *68,* 1853-1861.

21) Zeng, L.; Jiao, C.; Huang, K. W.; Chin, W. S.; Wu, J. Anthracene-fused BODIPYs as near-infrared dyes with high photostability. *Org. Lett.,* **2011,** *13,* 6026-6029.

22) Khakh, B. S.; Burnstock, G. The double life of ATP. *Sci. Am.,* **2009,** *301,* 84-92.

23) Castineira, J. R. P.; Garcia, R. G.; Marques, R. L. L.; Losada, M. Enzymatic systems of inorganic pyrophosphate bioenergetics in photosynthetic and heterotrophic protists: remmants or metabolic cornerstones? *Int Microbiol,* **2001,** *4,* 135-142.

24) Hu, M.; Feng, G. Highly selective fluorescent sensing of oxalate in water. *Chem. Commun.,* **2012,** *48,* 6951.

25) Bonizzoni, M.; Fabbrizzi, L.; Piovani, G.; Taglietti, A. Fluorescent detection of glutamate with a dicopper(II) polyamine cage. *Tetrahedron,* **2004,** *60,* 11159-11162.

26) Hu, P.; Yang, Yang, S.; Feng, G. Discrimination of adenine nucleotides and pyrophosphate in water by zinc complex of an anthracene-based cyclophane. *Org. Biomol. Chem.,* **2014,** *12,* 3701-3706.

27) Yadav, A.; Boomishankar, R. Concentration dependent ratiometric turn-on selective fluorescence detection of picric acid in aqueous and non-aqueous media. *RSC Advances,* **2013,** *5,* 3903-3907.

28) Zimmermann, Y.; Broekaert, J. A. J. Determination of TNT and its metabolites in water samples by voltammetric techniques. *Anal and Bioanal Chem,* **2005,** *383,* 998-1002.

29) Soltzberg, L. J.; Hagar, A.; Kridaratikorn, S.; Mattson, A.; Newman, R. MALDI-TOF mass spectrometric identification of dyes and pigments. *J. Am. Soc. Mass Spectrom,* **2007,** *18,* 2001-2026.

30) Joshi, S.; Kumari, S.; Chamorro, E.; Pant, D. D.; Sakhuja, R. Fluorescence quenching of a benzimidazolium–based probe for selective detection of picric acid in aqueous medium. *ChemistrySelect,* **2016,** *1,* 1756-1762.

31) Reddy, K. L.; Kumar, A. M.; Dhir, A.; Krishnan, V. New Ni-Anthracene complex for selective and sensitive detection of 2,4,6-trinitrophenol. *Int. J. Spectrosc,* **2018,** 1-5.

32) Mehrotra, P. Biosensors and their applications- A review. *J. Oral. Bio. Craniofac Res.,* **2016,** *6,* 153-159.

33) Soylemez, S.; Yılmaz, T.; Buber, E.; Udum, A. Y.; Özçubukçu, S.; Toppare, L. Polymerization and biosensor application of water soluble peptide-SNS type monomer conjugates. *J. Mater. Chem. B.*, **2017,** *5*, 7384-7392.

34) Mohanty, S. P.; Kougianos, E. Biosensors: A Tutorial Review. *IEEE Potentials,* **2006,** *25,* 35-40.

35) Ke, C.; Destecroix, H.; Crump, M. P.; Davis, P. A simple and accessible synthetic lectin for glucose recognition and sensing. *Nat Chem.*, **2012**, *4,* 718-723.

36) Polasek, M.; Caravan, P. Is macrocycle a synonym for kinetic inertness in Gd(III) complexes? Effect of coordinating and noncoordinating substituents on inertness and relaxivity of Gd(III) chelates with DO3A-like ligands. *Inorg. Chem.*, **2013,** *52*, 4084-4096.

37) Yu, K K.; Li, K.; Hou, J. T.; Yu, X. Q. Coumarin-TPA derivative: a reaction-based ratiometric fluorescent probe for Cu (I). *Tetrahedron Lett.*, **2013,** *54*, 5771-5774.

38) Mahbubul, A. Template synthesis of new type of macrocyclic molecule derived from pyridine -2,6-dicarboxaldehyde and 1,2-bis(2-aminoethoxy)ethane. *Journal of Bangladesh Academy of Sciences*, **2011,** *35*, 61-65.

39) Dong, Y. J.; Meng, Z. H.; Mi, Y. Q.; Zhang, C.; Cui, Z. H.; Wang, P.; Xu, Z. B. Synthesis of novel pleuromutilin derivatives. Part 1: P-preliminary studies of antituberculosis activity. *Bioorg. Med. Chem. Lett.*, **2015,** *25,* 1799-1803.

40) Kumari, S.; Joshi, S.; Sarmah, A.; Pant, D.; Sakhuja, R. Highly selective sensing of Li^+ in H_2O/CH_3CN via fluorescence 'turn-on' response of a coumarin-indole linked dyad: an experimental and theoretical study. *J. Fluoresc*, **2016,** *26,* 2177-2185.

41) Özil, M.; Canpolat, M. Solvent free synthesis of novel phthalocyanines containing triazole derivatives under microwave irradiation. *Polyhedron,* **2012,** *51,* 82-89.

42) Ekiz, F.; Oğuzkaya, F.; Akin, M.; Timur, S.; Tanyeli, C.; Toppare, L. Synthesis and application of poly-SNS-anchored carboxylic acid: a novel functional matrix for biomoleculeconjugation. *J. Mater. Chem.,* **2011,** *21,* 12337-12343.

43) Just, P. E.; Chane-Ching, K. I; Lacaze, P. C. Synthesis of 2,5-di(2-thienyl)-1H-pyrrole N-linked with conjugated bridges. *Tetrahedron,* **2002,** *58,* 3467-3472.

44) Truong, T. N. B.; Savagatrup, S.; Jeon, I.; Swager, T. M. Modular synthesis of polymers containing 2,5-di(thiophenyl)-N-arylpyrrole. *J. Polym. Sci. A. Poly. Chem.,* **2018,** *56,* 1133-1139.

APPENDICES

A. Appendix A

NMR DATA

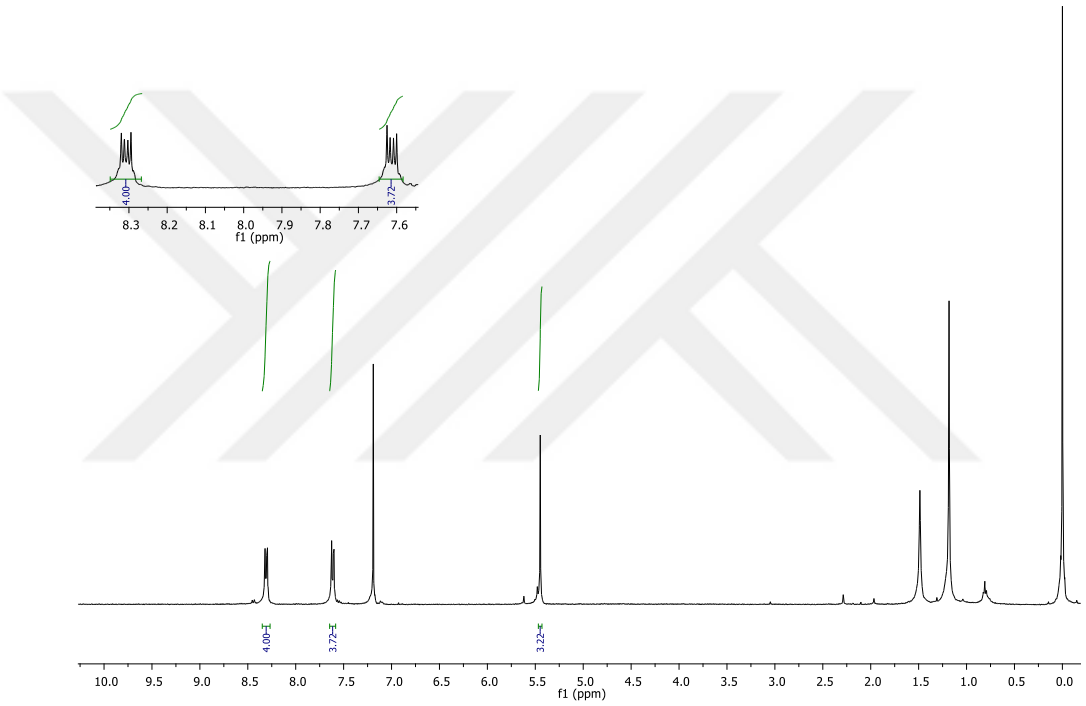

Figure A.1. ^{1}H NMR spectrum of 9,10-bis(bromomethyl)anthracene.

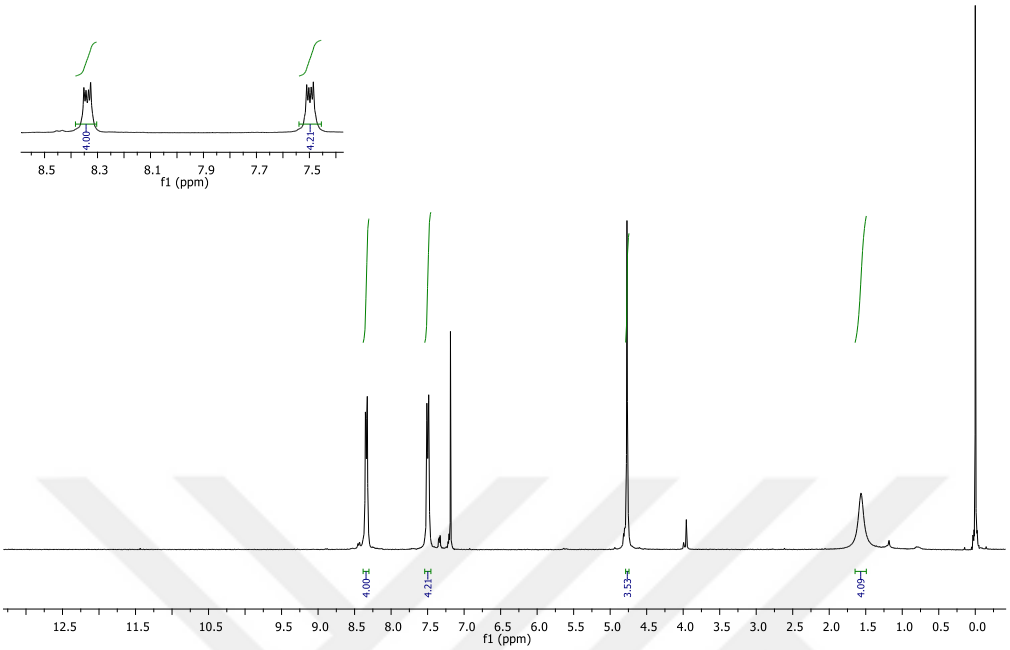

Figure A.2. ^{1}H NMR spectrum of 9,10-bis(aminomethyl)anthracene.

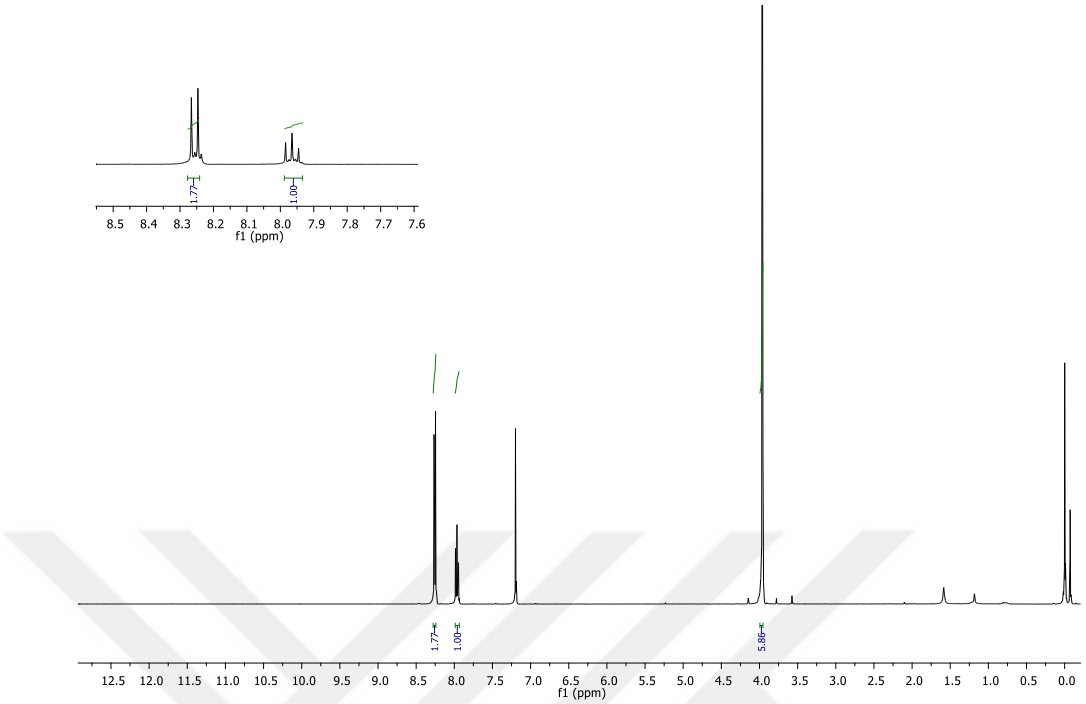

Figure A.3. ^{1}H NMR spectrum of dimethyl 2,6-pyridinedicarboxylate.

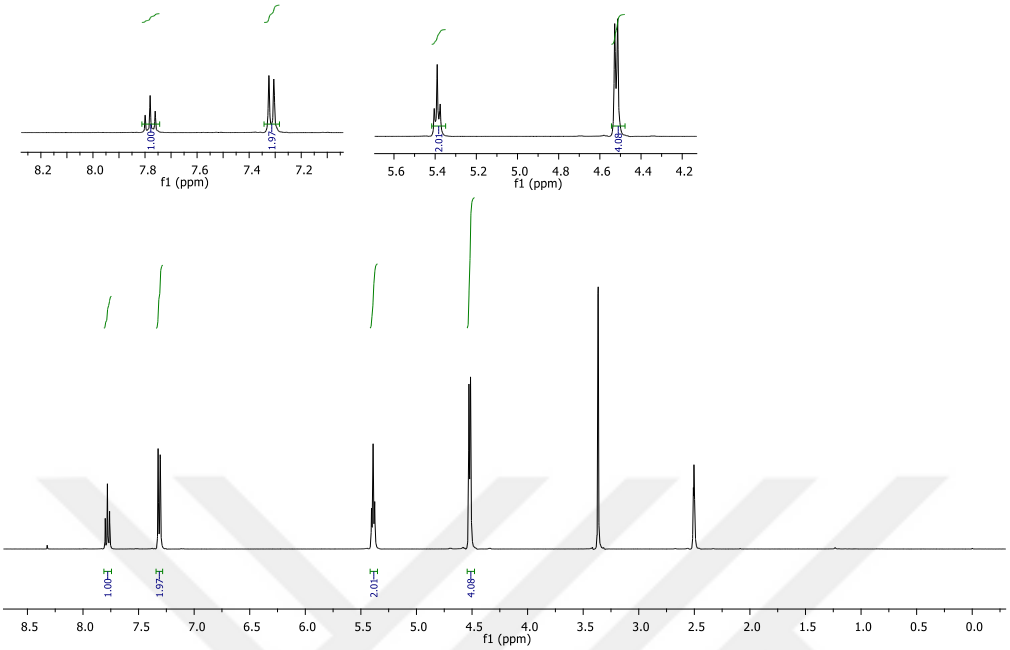

Figure A.4. ^{1}H NMR spectrum of 2,6-pyridinedimethanol.

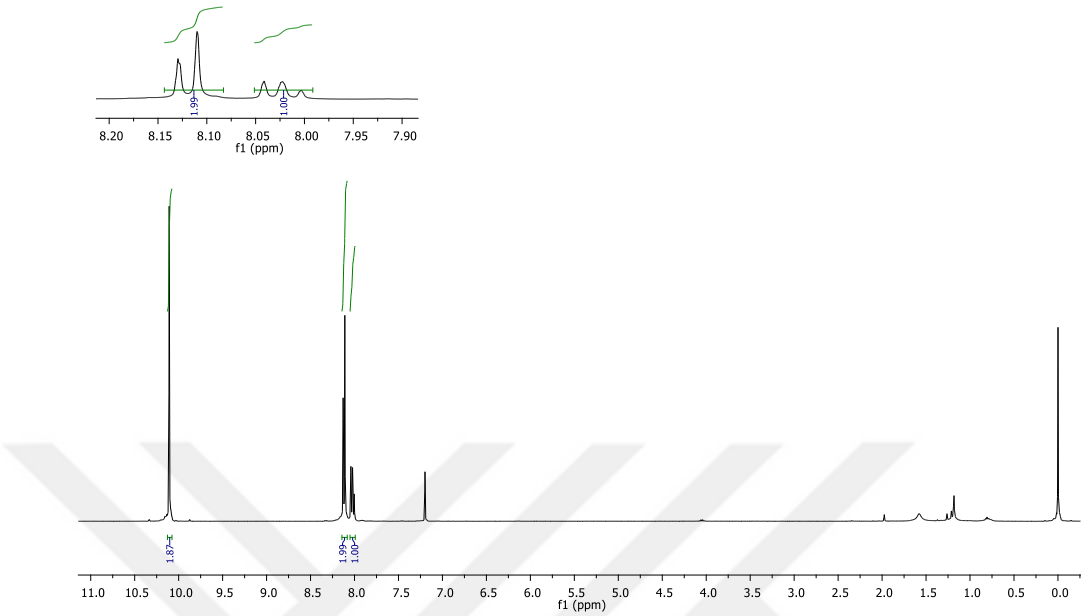

Figure A.5. ^{1}H NMR spectrum of 2,6-pyridinedicarboxyaldehyde.

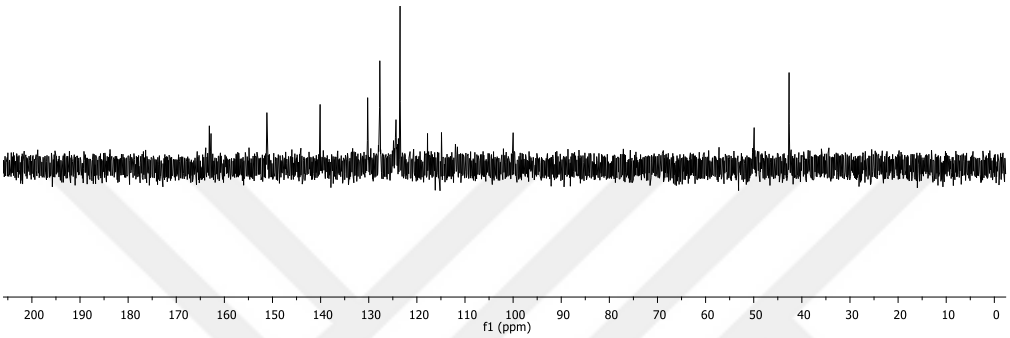

Figure A.6. ^{13}C NMR spectrum of compound **14**.

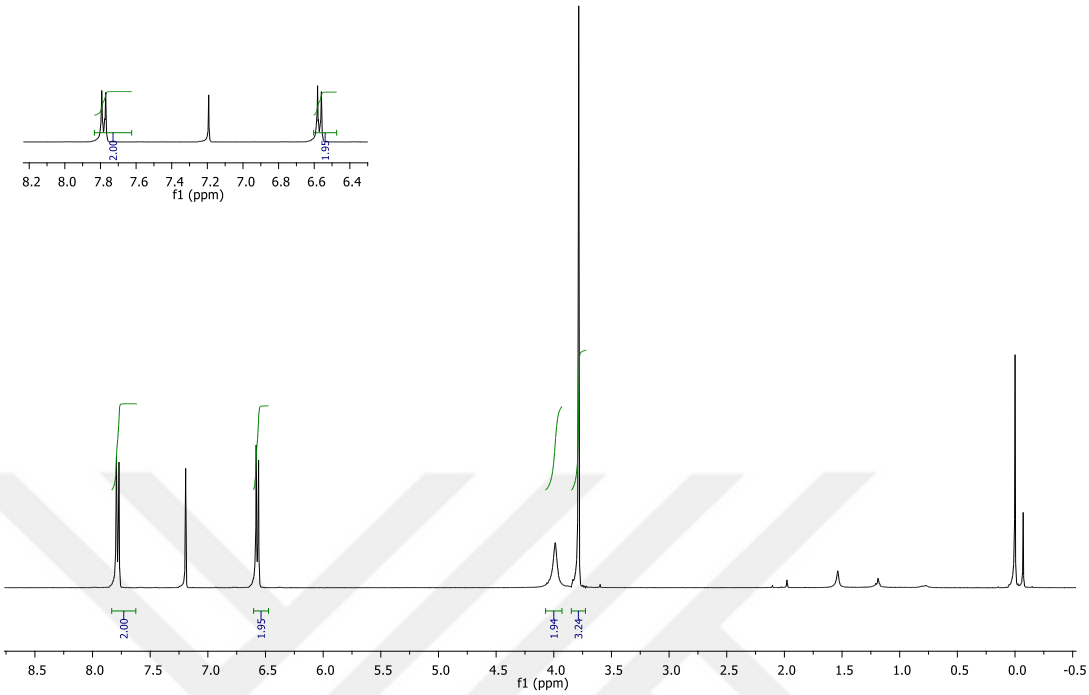

Figure A.7. . ^{1}H NMR spectrum of compound **32.**

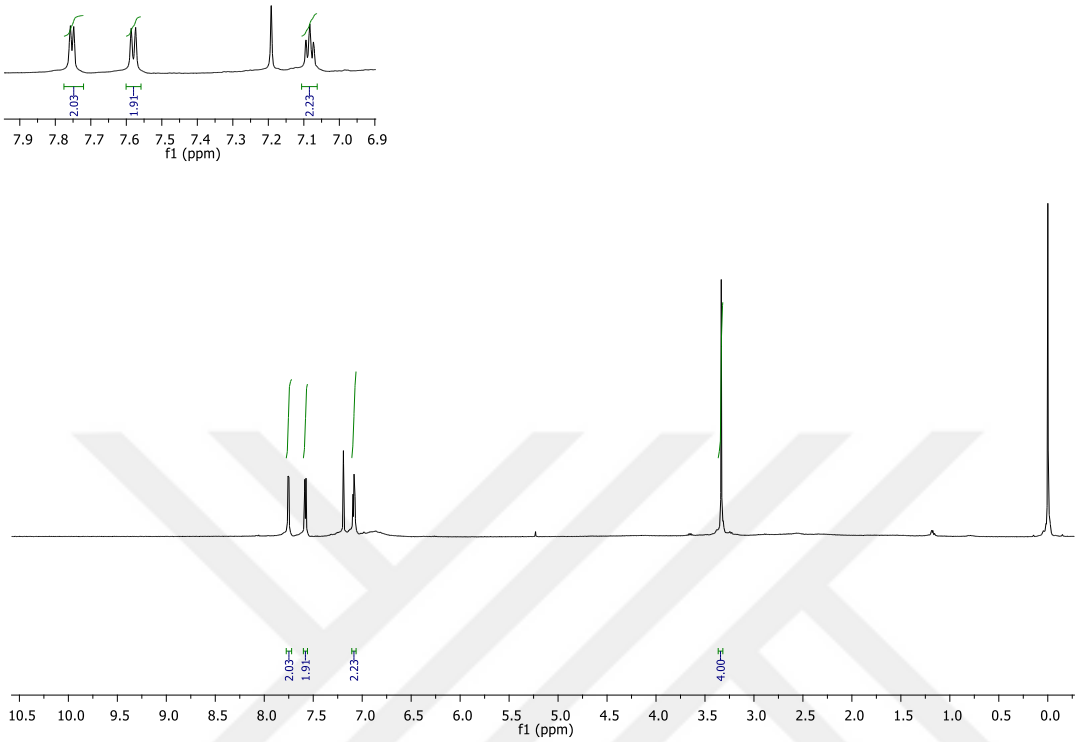

Figure A.8. . ^{1}H NMR spectrum of compound **33.**

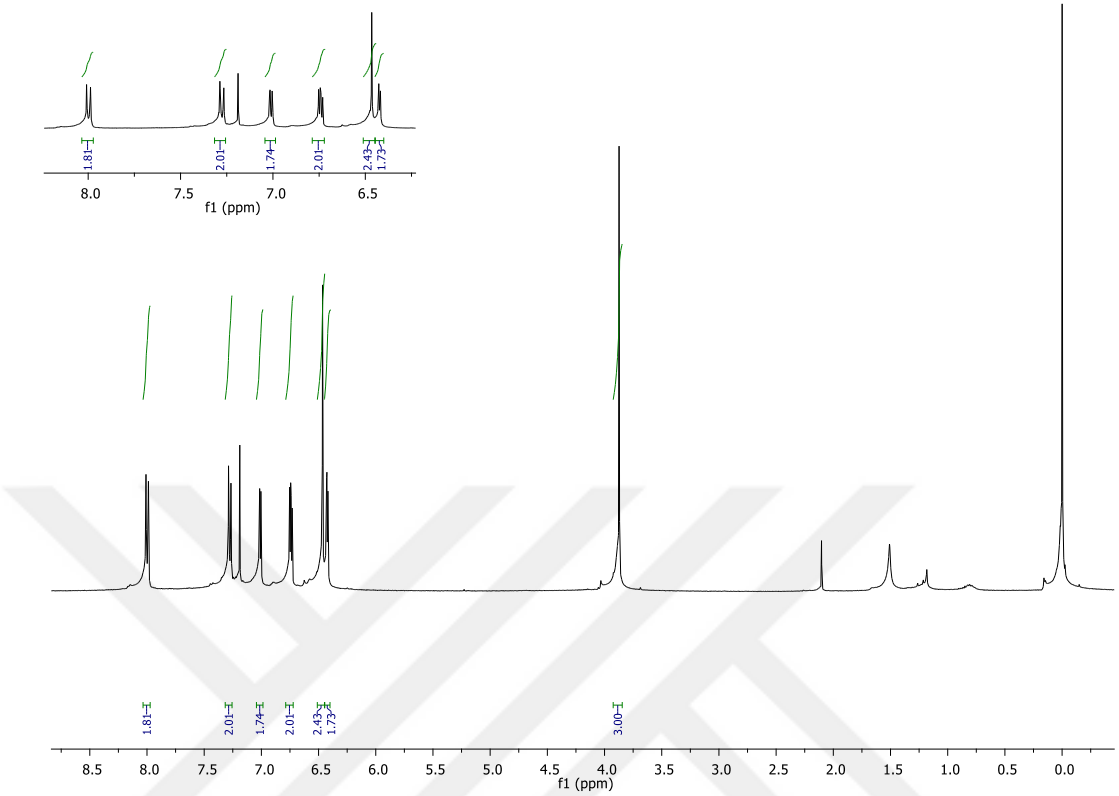

Figure A.9. ^{1}H NMR spectrum of compound **34**.

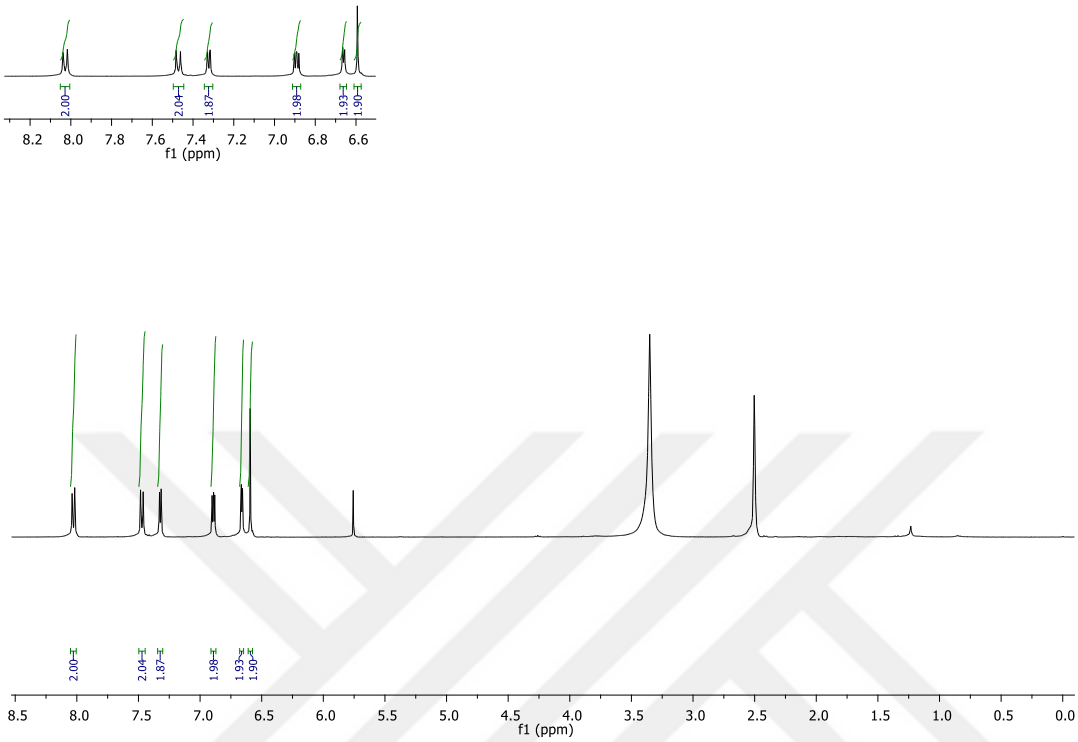

Figure A.10. ^{1}H NMR spectrum of compound **35**.

B. Appendix B

HRMS DATA

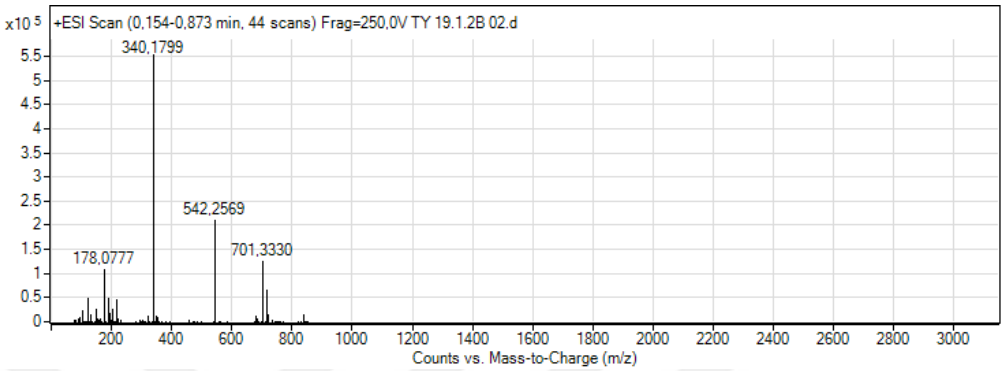

Figure B.1. HRMS chromatogram of **MC-1**.

C. Appendix C

HPLC DATA

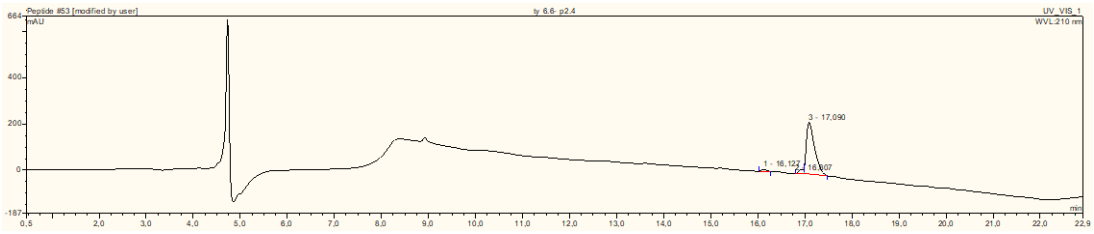

Figure C.1. HPLC chromatogram of compound **17.**

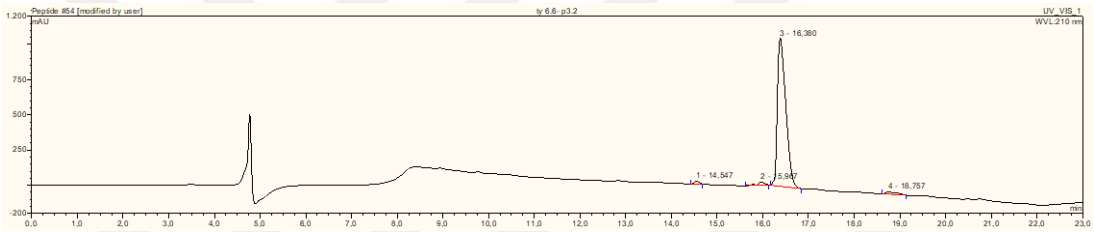

Figure C.2. HPLC chromatogram of compound **18.**